Heliyon 8 (2022) e09323

Contents lists available at ScienceDirect

Heliyon

journal homepage: www.cell.com/heliyon

Research article

Comparative lead adsorptions in synthetic wastewater by synthesized zeolite A of recycled industrial wastes from sugar factory and power plant

Sirirat Jangkorn [a,b], Sujittra Youngme [c], Pornsawai Praipipat [a,b,*]

[a] Department of Environmental Science, Faculty of Science, Khon Kaen University, Khon Kaen, 40002, Thailand
[b] Environmental Applications of Recycled and Natural Materials (EARN) Laboratory, Khon Kaen University, Khon Kaen, 40002, Thailand
[c] Materials Chemistry Research Center, Department of Chemistry, Khon Kaen University, Khon Kaen, 40002, Thailand

ARTICLE INFO

Keywords:
Bagasse fly ash
Coal fly ash
Zeolite
Batch study
Heavy metal

ABSTRACT

Increasing of industrializations causes of waste management problems, so use of industrial wastes for other purposes is an alternative option not only reducing industrial wastes but also providing benefit applications. Water contaminated by heavy metals is concerned because of their toxicity, so the water treatment is required. Sugar factory and power plant create big loads of wastes which are bagasse fly ash (BFA) and coal fly ash (CFA). Since BFA and CFA have good chemical properties, they are possible to apply as raw materials for synthesis of zeolite–type adsorbents. Thus, use of these industrial wastes for heavy metal adsorptions is a good idea to accomplish for the waste management and water quality. This study presented the modified method of zeolite A synthesis by BFA and CFA for lead removals, characteristic identifications of synthesized zeolite A adsorbents, their lead adsorption efficiencies, and their adsorption isotherm and kinetics were investigated. ZBG and ZCF were synthesized, and all analytic characterizations were determined that ZBG and ZCF corresponded to zeolite A standard (STD). ZBG and ZCF were demonstrated lead removal efficiencies of 100%. The highest negatively charged of ZBG and ZCF were found at pH of 5 matched to the highest lead removal efficiencies of both zeolite A adsorbents. Adsorption isotherms and kinetics of ZBG and ZCF were corresponded to Langmuir isotherm and pseudo-second-order kinetic model. Therefore, ZBG and ZCF are potential adsorbents for environmental applications along with reducing of industrial wastes.

1. Introduction

Releasing of industrial wastewaters contaminated with heavy metals such as mercury, lead, cadmium, chromium is concerned because of their toxicity, persistence, and bioaccumulation to organisms through food chains [1,2]. Especially, lead is one of top three highly toxic heavy metals because it potential damages to human functional systems of central nervous, brain function, reproductive [3]. The source of lead discharging to the environment may be from industries of batteries, steels, pigments, paints, and plastic [4,5], so their effluents are necessary to treat before discharging to the receiving water which the lead concentration is required under 0.2 mg/L following USEPA standard [6].

Although chemical precipitation, oxidation-reduction, ion-exchange, membrane filtration, reverse osmosis are commonly used for heavy metal removals in wastewater [7,8], these methods have disadvantages of high operating costs, complicated operations, high energy-requiring [8,9]. While the adsorption may be a good offer with the simple and effective method including of reasonable cost for lead removal in wastewater [10]. Various types of commercial, natural, and wastes adsorbents are generally applied for lead removal in wastewater, and some previous studies were reported in Table 1. Activated carbon, carbon foam, and zeolite A are represented as commercial adsorbents, and natural adsorbents are fava beans, natural zeolite, and cocoa pod husk. Many types of agricultural waste adsorbents of oil palm frond, watermelon rind, herbaceous weed, coconut leaves, potato peel, pineapple peel fiber, food waste adsorbents of jackfruit peel activated carbon, eggshells, orange peel and industrial waste adsorbents of paper sludge, stainless steel slag, grape stalk waste, bagasse fly ash, coal fly ash are interesting choices for reducing of waste disposal loads by using of wastes as low-cost adsorbents along with improving of the water quality. Among these waste adsorbents, the industrial wastes of bagasse fly ash (BFA) and coal fly ash (CFA) which are large amounts of solid waste of sugar factory and power plant [11] are good options because using of these industrial wastes in

* Corresponding author.
E-mail address: pornprai@kku.ac.th (P. Praipipat).

https://doi.org/10.1016/j.heliyon.2022.e09323
Received 5 August 2021; Received in revised form 26 February 2022; Accepted 20 April 2022

Table 1. A summary of lead adsorptions on various types of adsorbents.

Adsorbent	Type of adsorbent	Conditions					Results		Reference
		Dose (g)	Contact time (min)	pH	Concentration (mg/L)	Volume (mL)	q_m (mg/g)	Removal (%)	
Activated carbon	Commercial	5	1,440	-	50	250	1428.57	98	[16]
Carbon foam	Commercial	0.03	1,440	7.0	50	200	460.50	73.99	[17]
Zeolite A	Commercial	0.15	40	4.0	100	50	-	51.60	[18]
Fava Beans	Natural	0.002	40	4.5	1.23	200	-	27.64	[19]
Natural zeolite	Natural	1,000	1,440	5.2	1,375	50	14.25	-	[20]
Cocoa pod husk	Natural	-	120	6.0	-	-	20.10	-	[21]
Oil palm frond	Agricultural waste	2	-	3.0	100	50	5.32	-	[22]
Watermelon rind	Agricultural waste	-	-	5.0–6.8	-	-	98.06	99	[23]
Herbaceous weed	Agricultural waste	-	120	6.0	-	-	-	78	[24]
Coconut Leaves	Agricultural waste	0.003	40	4.5	1.23	200	-	26.01	[19]
Potato peel	Agricultural waste	-	-	6.0	-	-	-	92	[25]
Pineapple peel fiber	Agricultural waste	-	-	5.6	-	-	70.29	-	[26]
Jackfruit peel activated carbon	Food-waste	5	1,440	-	50	250	1,000	80	[16]
Eggshells	Food-waste	0.3	50	9.5	400	350	923	-	[27]
Orange peel	Food-waste	-	-	-	-	-	209.80	-	[28]
Paper sludge	Industrial waste	0.1	1,440	6.5	460	10	-	100	[29]
Stainless steel slag	Industrial waste	0.1	240	9.0	10	10		>95	[30]
Grape stalk waste	Industrial waste	0.1	-	5.5	0.241	15	0.241	-	[31]
Bagasse fly ash	Industrial waste	-	-	-	-	-	-	95–96	[32]
Coal fly ash	Industrial waste	-	-	-	-	-	0.22	-	[33]

other benefit purposes can resolve waste disposal problems along with idea of reducing demand of raw materials.

The main chemical elements of BFA and CFA are silicon (Si), aluminum (Al), and oxygen (O), and they also have four main chemical compounds which are silicon dioxide (SiO_2), aluminum oxide (Al_2O_3), iron (III) oxide (Fe_2O_3), and calcium oxide (CaO) with weight percentage of 20.85 wt%, 4.23 wt%, 5.25 wt% and 63.49 wt%, respectively for BFA [12], and 35.43 wt%, 22.82 wt%, 11.47 wt% and 20 wt%, respectively for CFA [13]. Therefore, they are suitable raw materials for possibly synthesis of zeolite-type adsorbents for heavy metal adsorptions in wastewater [14]. In case of heavy metal adsorbents, zeolite type A is preferred because of its good characteristics of microporous and numerous cavities [15], so it may obtain a high adsorption efficiency which zeolite A was also widely applied for heavy metal removals such as lead (Pb), cadmium (Cd), zinc (Zn), calcium (Ca) and copper (Cu) in many studies reported in Table 2. In Table 2, various raw materials of kaolin, textile waste ash, fly ash, and bagasse fly ash have been used for zeolite A synthesis with different synthesized methods of hydrothermal treatment and alkaline fusion, and their results also reported high adsorptions of heavy metals more than 95%. Therefore, it is possible to use waste materials of BFA and CFA for zeolite A synthesis and apply for lead removals in this study.

Two main steps of silicon (Si) and aluminum (Al) extractions by alkaline fusion method and zeolite synthesis by hydrothermal method are commonly recommended for zeolite synthesis [16–22]. However, a raw material is a key factor affecting to the quality of synthesized zeolite

Table 2. A summary of heavy metal adsorptions on zeolite A synthesized by various raw materials.

Raw material	Synthesis method	Conditions						Results		Reference
		Heavy metals	Dose (g)	Contact time (min)	pH	Concentration (mg/L)	Volume (mL)	q_m (mg/g)	Removal (%)	
Kaolin	Hydrothermal treatment	Pb^{2+}	0.40	30	-	100	-	-	96	[34]
Kaolin	Alkaline fusion	Pb^{2+}	0.07	60	6.5	0.05	25	14.64	-	[35]
Kaolin	Alkaline fusion and Hydrothermal	Pb^{2+}	0.40	30	7.5	-	-	-	-	[36]
		Cd^{2+}	0.80							
		Cu^{2+}	0.80							
		Zn^{2+}	0.80							
		Ni^{2+}	0.80							
Textile Waste Ash	Hydrothermal treatment	Pb^{2+}	1.00	30	-	100	100	-	98–90	[37]
Fly ash	Alkaline fusion and Hydrothermal	Ca^{2+}	5.00	30	-	-	-	-	95	[38]
Bagasse fly ash	Hydrothermal	Cu^{2+}	-	-	-	-	-	142	-	[39]

because of the different chemical compositions in a raw material. Therefore, a raw material is the first factor to consider before selecting of zeolite synthesis method to achieve high purity of zeolite adsorbent. The pretreatment of raw material is another important process to eliminate contaminated elements before synthesis of zeolite, and its method also depends on a raw material. Therefore, this study proposed the method modifications of synthesis zeolite from two industrial wastes to accomplish high quality of zeolite A adsorbents with possibly perfect cubic shape for environmental applications in the wastewater treatment.

In the present study, an attempt presented the effective zeolite A adsorbents by using of industrial wastes of sugar factory and power plant as low-cost adsorbents for lead removals in the aqueous solution to achieve both the water quality and waste management. The crystalline formations, surface morphologies, chemical compositions, chemical functional groups, size of surface area, pore size, and pore volume of synthesized zeolite A adsorbents were examined. The influences of dose, contact time, pH, and concentration for lead adsorptions by zeolite A adsorbents were investigated and compared by batch experiments. The surface charge of zeolite A materials were also investigated by zeta potential experiments. The adsorption equilibrium and adsorption mechanism of adsorbed leads on zeolite A adsorbents were also studied through adsorption isotherm and kinetic experiments.

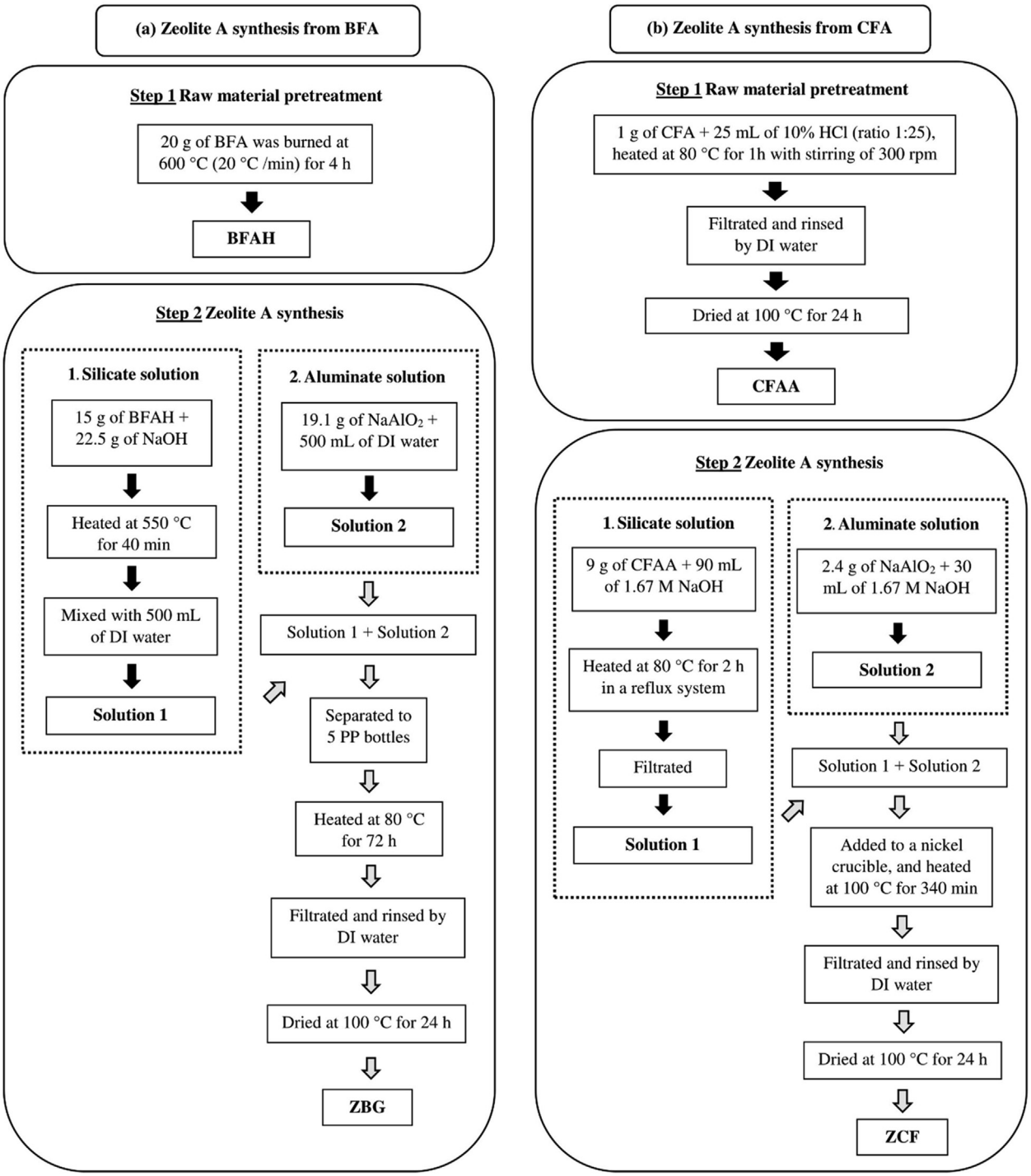

Figure 1. Flow diagrams of zeolite A synthesis from (a) BFA and (b) CFA.

2. Materials and methods

2.1. Raw materials

Bagasse fly ash (BFA) and coal fly ash (CFA) were used as raw materials for this study. BFA was collected from a sugar factory located Khon Kaen province, Thailand, and CFA was collected from Mae Moh Power Plant, Lumpang provice, Thailand.

2.2. Chemicals

All reagents were analytical grades (AR) which were used without the purification. 37% Hydrochloric acid (HCl) (RCI Labscan, Thailand) was used for the pretreatment of coal fly ash. Sodium hydroxide (NaOH) (RCI Labscan, Thailand) and sodium aluminate ($NaAlO_2$) (Sigma-Aldrich, Germany) were used for zeolite synthesis. Lead nitrate ($Pb(NO_3)_2$) (QRëC, New Zealand) was used for the synthetic wastewater preparation. 1% Sodium hydroxide (NaOH) (RCI Labscan, Thailand) and 1% nitric acid (HNO_3) (Merck, Germany) were used for pH adjustments. Finally, commercial zeolite A (Sigma-Aldrich, Germany) was used as representative zeolite A standard (STD).

2.3. Zeolite A synthesis

The details of zeolite A synthesis from BFA and CFA were demonstrated in Figure 1a-b, and were clearly explained step by step below:

2.3.1. Zeolite A synthesis from BFA

Zeolite A synthesis from BFA consisted of two steps which were the raw material pretreatment and zeolite A synthesis shown in Figure 1a. The purpose of pretreatment step by calcinations at 600 °C was to remove the contaminated elements such as rubidium (Rb), chromium (Cr), copper (Cu), chlorine (Cl) from a raw material in order to increase the mass of silicon (Si) element for zeolite A synthesis [40]. For zeolite A synthesis, the modified method from Moisés et al., 2013 [41] by alkaline fusion method followed by hydrothermal method was applied in this study. The details of two steps were explained below:

Step 1: Raw material pretreatment, 20 g of BFA were added to 50 mL of ceramic crucible and were burned by a multistage programmable furnace (Vulcan, 3-1750, Canada) at 600 °C for 4 h with an increasing of temperature with the ratio of 20 °C /min. Then, they were kept in desiccators until use called BFAH.

Step 2: Zeolite A synthesis, the first process of zeolite A synthesis is the stage of silicon (Si) and aluminum (Al) extractions, so the silicate solution and aluminate solution are needed to prepare prior to the stage of zeolite A synthesis by the hydrothermal method.

For the preparation of silicate solution by alkaline fusion method, 15 g of BFAH and 22.5 g of NaOH were added to a nickel crucible (United Scientific, NCR100, USA) and were heated by a furnace (Carbolite, CWF, England) at 550 °C for 40 min. Then, the sample was added to 1000 mL of Beaker which contained 500 mL of DI water and was mixed by a magnetic stirrer of 200 rpm for 30 min called solution 1. For the aluminate solution, 19.1 g of $NaAlO_2$ and 500 mL of DI water were added in 1000 mL of Beaker and were mixed by a magnetic stirrer of 200 rpm for 30 min called solution 2.

For zeolite A synthesis, solution 2 was slowly added to 1000 mL of Beaker that contained solution 1 with mixing continuously by a magnetic stirrer of 200 rpm for 30 min. This process is a significant point to achieve a good cubic shape of zeolite A. Then, the mixed solution was separated to five 250 mL polypropylene (PP) bottles for the volume of 200 mL per each, and then they were heated in a hot air oven at 80 °C for 72 h for the zeolite formation. Next, they were filtrated by a glass microfiber filter (GF/C) which connected to a vacuum pump and were rinsed by DI water. Finally, the filtrated sample was dried by a hot air oven (Binder, FED 53, Germany) at 100 °C for 24 h and was kept in desiccators until use called ZBG.

2.3.2. Zeolite synthesis from CFA

Zeolite A synthesis from CFA also consisted of two steps which were the raw material pretreatment and zeolite A synthesis shown in Figure 1b. The purpose of pretreatment step by an acid washing method was the purification of raw material and increasing of mainly mass of silicon (Si) element for zeolite A synthesis by removing of contaminated elements such as copper (Cu), sodium (Na), chlorine (Cl), arsenic (As) [42]. For zeolite A synthesis, the modified method from Wang et al., 2008 [43] by alkaline fusion method followed by hydrothermal method was applied in this study. The silicate solution preparation and zeolite A formation in a hydrothermal part were modified in this study. For the preparation of silicate solution, the heating equipment was changed from a water bath at 80 °C to a reflex system at 80 °C with white oil solution because of its good controlling of constant temperature and keeping a final silicate solution volume. For the hydrothermal process, the sample container was changed from a stainless alloy autoclave to a nickel crucible because of its suitable property of strong base with a reasonable budget. The details of two steps were explained below:

Step 1: Raw material pretreatment, the ratio of 1 g CFA to 25 mL of 10% HCl solution was applied for the raw material pretreatment. For example, 1 g of CFA was washed by adding to 25 mL of 10% HCl solution in 125 mL of Erlenmeyer flask. Next, the mixed solution in Erlenmeyer flask was soaked in 500 mL of Beaker that contained 300 mL of distilled water and was heated by a hot plate (IKA, C-MAG HS 7, Malaysia) at 80 °C with continuous stirring of 300 rpm for 1 h. Then, the sample was filtrated by a glass microfiber filter and was rinsed by DI water. Finally, the filtrated sample was dried by a hot air oven at 100 °C for 24 h and was kept in desiccators until use called CFAA.

Step 2: Zeolite A synthesis, the silicate solution and aluminate solution were also prepared by alkaline fusion method. For the silicate solution, 9 g of CFAA and 90 mL of 1.67 M NaOH were added to 150 mL of round bottom flask, and then it was soaked in 1L of glass bowl container that contained 500 mL of white oil in a reflux system at 80 °C with continuous stirring of 300 rpm for 2 h. This process was important to obtain the stable temperature and final silicate volume. Finally, the mixed solution was filtrated by a glass microfiber filter called solution 1. For the aluminate solution, 2.4 g of $NaAlO_2$ were added to 100 mL of Beaker that contained 30 mL of 1.67 M NaOH and were mixed by a magnetic stirrer of 200 rpm for 30 min called solution 2.

For zeolite A synthesis, solution 1 and 2 were added to 250 mL of Beaker and were mixed by a magnetic stirrer of 200 rpm for 30 min. Then, the mixed solution was added to 150 mL of nickel crucible and was heated by a hot air oven at 100 °C for 340 min. Next, the mixed solution was filtrated by a glass microfiber filter and was rinsed by DI water. Finally, the filtrated sample was dried by a hot air oven at 100 °C for 24 h and was kept in desiccators until use called ZCF [43].

2.4. Characterizations of synthesized zeolites

X-ray diffractometer (XRD) (PANalytical, EMPYREAN, United Kingdom) in the range of $2\theta = 5\text{-}45^\circ$ was used to identify the crystalline formations of zeolite A adsorbents. The surface morphologies of zeolite A adsorbents were studied by Scanning electron microscopy (SEM) technique which was carried out on Field Emission Scanning Electron Microscopy and Focus Ion Beam (FESEM-FIB) (FEI, Helios NanoLab G3 CX, USA). The X-ray fluorescence (XRF) technique which was carried out on Rigaku wavelength dispersive X-ray fluorescence (WD-XRF) (Rigaku, ZSX Primus II, Tokyo) was used to determine the element compositions in mass percentage of zeolite A adsorbents. Fourier Transform Infrared (FTIR) spectroscopy (Thermo Fisher Scientific, Nicolet 6700, USA) was used to investigate chemical functional groups of zeolite A adsorbents. The size of surface area, pore volume, and pore size of zeolite A adsorbents were analyzed by Brunauer-Emmett-Teller (BET) technique by isothermal nitrogen gas (N_2) adsorption in the surface area & pore size analyzer (Quantachrome instrument, QUADRASORB evo™, AUSTRIA). Finally, the zeta potentials of zeolite A adsorbents were examined by the

laser zetameter (Malvern Instruments, Zetasizer Nano ZS system, United Kingdom).

2.5. Batch adsorption experiments

Batch adsorption experiments were designed to investigate the effects of dose, contact time, pH and concentration on lead removal efficiencies of ZBG and ZCF. Atomic Adsorption Spectrophotometer (AAS) (PerkinElmer, PinAAcle 900F, USA) was used for analyzing lead concentrations in all samples. The details of batch adsorption experiments were explained below:

2.5.1. Effect of dose

Lead removal efficiencies of ZBG and ZCF were investigated with seven different dosages of 0.005 g, 0.010 g, 0.015 g, 0.020 g, 0.025 g, 0.030 g and 0.035 g and the control condition of sample volume of 200 mL, lead concentration of 50 mg/L, shaking speed of 200 rpm, contact time for 5 h, and pH 5 to find the optimum adsorbent dosage of ZBG and ZCF. The lowest adsorbent dosages of ZBG and ZCF with the highest lead removal efficiencies were chosen as the optimum dose and were used to study the effect of contact time.

2.5.2. Effect of contact time

Lead removal efficiencies of ZBG and ZCF were studied with five different contact time values of 1, 2, 3, 4 and 5 h and the control condition of sample volume of 200 mL, lead concentration of 50 mg/L, shaking speed of 200 rpm, pH 5, and the optimum doses of ZBG and ZCF from 2.5.1 to investigate the optimum contact time of ZBG and ZCF. The lowest contact time of ZBG and ZCF with the highest lead removal efficiencies were chosen as the optimum contact time and were used to study the effect of pH.

2.5.3. Effect of pH

Lead removal efficiencies of ZBG and ZCF were studied with six pH values of 1, 3, 5, 7, 9 and 11 which were representative acid, neutral, and base conditions and the control condition of sample volume of 200 mL, lead concentration of 50 mg/L, shaking speed of 200 rpm, and the optimum doses and contact time of ZBG and ZCF from 2.5.1 and 2.5.2 to examine the optimum pH of ZBG and ZCF. Although an acid condition is normally preferred for lead adsorption of many adsorbents [44], zeolite A adsorbents also need to investigate possibly lead adsorption in a strong acid or base condition of real wastewater applications such as battery industry wastewater for a strong acid condition of pH 1-2 [45,46] or textile industrial wastewater for a strong base condition of pH 9-11 [47]. The pH values of ZBG and ZCF with the highest lead removal efficiencies were chosen as the optimum pH and were used to study the effect of concentration.

2.5.4. Effect of concentration

Lead removal efficiencies of ZBG and ZCF were studied with seven concentrations of 10, 20, 30, 40, 50, 60 and 70 mg/L and the control condition of sample volume of 200 mL, shaking speed of 200 rpm, and the optimum dose, contact time, and pH from 2.5.1, 2.5.2, and 2.5.3 to explore the optimum concentrations of ZBG and ZCF. The concentrations of ZBG and ZCF with the highest lead removal efficiencies were chosen as the optimum concentration.

The percentage of lead removal efficiency and lead adsorption capacity of zeolite A adsorbent were calculated by Eqs. (1) and (2): [48, 49, 50].

$$\text{Lead removal efficiency (\%): \%Removal} = (C_0–C_e)/C_0 \text{ x } 100 \quad (1)$$

$$\text{Lead adsorption capacity: } q_e = (C_0–C_e)V/m \quad (2)$$

where C_e is the equilibrium of lead concentration in the solution (mg/L), and C_0 is the initial lead concentration (mg/L), q_e is the amount of adsorbed lead on zeolite A adsorbent (mg/g), V is the sample volume (L), and m is the amount of zeolite A adsorbent (g).

2.6. Adsorption isotherms

Adsorption isotherm can be used to describe the interaction of lead solution with zeolite A adsorbent which is normally analyzed by using Langmuir and Freundlich isotherms following Eqs. (3) and (4) [50].

$$\text{Langmuir isotherm: } C_e/q_e = 1/q_m b + C_e/q_m \quad (3)$$

$$\text{Freundlich isotherm: } \log q_e = \log K_F + 1/n \ (\log C_e) \quad (4)$$

where C_e is the equilibrium of lead concentration (mg/L), q_e is the amount of lead adsorbed on zeolite A adsorbent (mg/g), q_m is the maximum amount of lead adsorption on zeolite A adsorbent (mg/g), b is the adsorption constant (L/mg), K_F is the constant of adsorption capacity (mg/g) and $1/n$ is the constant depicting of the adsorption intensity.

For adsorption isotherm experiments, 0.02 g of ZBG or ZCF were added to 250 mL Erlenmeyer flasks with lead concentrations from 10 mg/L to 70 mg/L. The control conditions of ZBG and ZCF were the sample volume of 200 mL, contact time for 2 h of ZBG and 1 h of ZCF, pH 5, and shaking speed of 200 rpm.

2.7. Adsorption kinetics

The adsorption mechanism of lead adsorption on zeolite A adsorbent can be described by adsorption kinetics. Characteristic constants of adsorbent materials were investigated by using pseudo-first order (PFO) and pseudo-second order (PSO) kinetic models following Eqs. (5) and (6), respectively [27,51].

$$\text{Pseudo-first-order kinetic model (PFO): } \ln (q_e - q_t) = \ln q_e - k_1 t \quad (5)$$

$$\text{Pseudo-second-order kinetic model (PSO): } t/q_t = t/q_e + 1/(k_2 q_e^2) \quad (6)$$

where q_e is the amount of adsorbed lead on zeolite A adsorbents (mg/g), q_t is the amount of adsorbed lead at time t (mg/g), k_1 and k_2 are pseudo-first order rate constant (min^{-1}), and pseudo-second order rate constant ((g/mg min), respectively.

For adsorption kinetic experiments, 0.1 g of ZBG or ZCF were added to 1000 mL of Breaker with lead concentration of 50 mg/L. The control condition of ZBG and ZCF was the sample volume of 1000 mL, contact time for 5 h, pH 5, and shaking speed of 200 rpm.

3. Results and discussion

3.1. Characterizations of zeolite A adsorbents

3.1.1. The physical characterization of materials

The physical characterizations of raw materials (BFA and CFA), raw materials with pretreatment (BFAH and CFAA), synthesized zeolite A adsorbents (ZBG and ZCF), and zeolite A standard (STD) were represented in Figure 2a-g. For raw materials, BFA was fine black color powder shown in Figure 2a which a black color indicated a high content of carbon compounds [52] whereas CFA was fine brown color powder shown in Figure 2b which a brown color demonstrated iron and carbon cannot completely be burned from coal fly ash [53]. For raw materials with pretreatment, BFAH was changed to brown color powder shown in Figure 2c which might be from the calcination process resulted in the decreasing of carbon content in a raw material [54]. CFAA was changed to gray color powder shown in Figure 2d which it might result from the removing of pollutants in a coal fly ash out after the pretreatment process [54,55]. For synthesized zeolite A adsorbents, ZBG was fine cream color powder shown in Figure 2e whereas ZCF was fine white powder shown in Figure 2f. Finally, only physical characteristic of ZCF was similarly to STD shown in Figure 2g with white color powder.

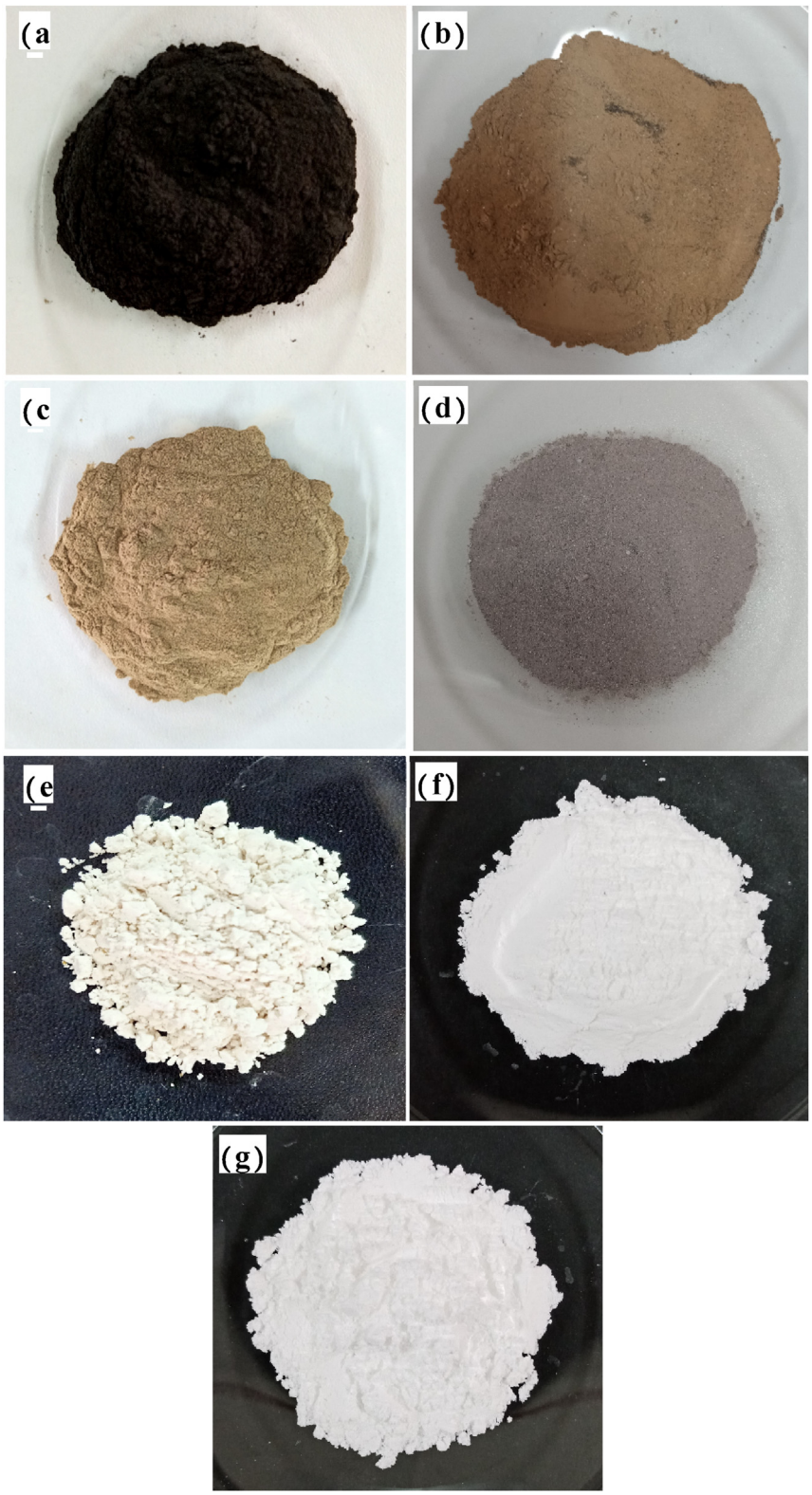

Figure 2. The physical characterizations of (a) BFA, (b) CFA, (c) BFAH, (d) CFAA, (e) ZBG, (f) ZCF, and (g) STD.

3.1.2. Physiochemical properties

The physiochemical properties of raw materials (BFA, CFA), raw materials with pretreatment (BFAH, CFAA), and the synthesized zeolite A adsorbents (ZBG, ZCF) and zeolite A standard (STD) were reported in Table 3. Three physical properties of all materials in size of surface area, pore volume, and pore size were determined by using Brunauer-Emmet and Teller technique with N_2 adsorption-desorption isotherm at 77.3 K and degas temperature of 80 °C for 6 h, and the results realized the significant changing values of three physical properties after the pre-treatment process. The size of surface area, pore volume and pore size were reported by multipoint BET, total pore volume for pore with Radius, and average pore radius, respectively. For BFA and BFAH, size of surface

Table 3. Physicochemical property of BFA, BFAH, ZBG, CFA, CFAA, ZCF and STD by BET analysis.

Physical properties	BFA	BFAH	ZBG	CFA	CFAA	ZCF	STD
Surface area (m^2/g)	36.870	10.230	1.548	1.390	97.680	10.440	10.460
Pore volume (cc/g)	0.067	0.052	0.005	0.006	0.086	0.030	0.030
Pore size (Å)	36.800	102.000	61.140	79.690	17.540	55.750	49.020
Chemical properties in chemical composition (wt% by mass)							
SiO_2	72.80	74.50	47.20	22.10	96.20	52.80	42.50
Al_2O_3	9.16	9.41	38.40	12.10	6.01	33.80	37.00
Fe_2O_3	5.05	4.57	0.08	15.00	17.20	0.13	0.02
CaO	3.34	2.99	0.09	32.60	2.23	0.09	0.06
MgO	1.47	1.50	0.23	1.99	1.69	0.00	0.27
Na_2O	0.00	0.00	0.00	1.82	0.00	12.4	20.00
K_2O	3.84	3.46	0.68	1.78	1.71	0.65	0.07
SO_3	1.34	1.02	0.03	11.2	0.57	0.00	0.02
P_2O_5	1.72	1.62	0.16	0.38	0.12	0.08	0.10
TiO_2	0.66	0.53	0.00	0.38	0.27	0.00	0.00
MnO	0.27	0.25	0.05	0.19	0.07	0.00	0.00

area, pore volume, and pore size of BFA were 36.870 m^2/g, 0.067 cc/g, and 36.800 Å, respectively whereas size of surface area, pore volume, and pore size of BFAH were 10.230 m^2/g, 0.052 cc/g, and 102.000 Å, respectively. As a result, the pretreatment process of BFA by calcinations affected to decrease the surface area and pore volume whereas pore size was increased which the decreasing of surface area might result from eliminated carbon from BFA [52]. As a result, zeolitic minerals were formed after eliminated carbon by the calcination process [39]. For CFA and CFAA, size of surface area, pore volume, and pore size of CFA were 1.390 m^2/g, 0.006 cc/g, and 79.690 Å, respectively whereas size of surface area, pore volume, and pore size of CFAA were 97.680 m^2/g, 0.086 cc/g, and 17.540 Å, respectively. As a result, the pretreatment process of CFA affected to highly increase the surface area and pore volume whereas pore size was decreased because of eliminated contaminants and organic compounds from the outer layer surface of CFA by HCI [56,57]. Therefore, the pretreatment process is an important step to purify raw material before zeolite A synthesis.

For zeolite A adsorbents (ZBG and ZCF), size of surface area, pore volume, and pore size of ZBG were 1.548 m^2/g, 0.005 cc/g, and 61.140 Å, respectively whereas size of surface area, pore volume, and pore size of ZCF were 10.440 m^2/g, 0.030 cc/g, and 55.750 Å, respectively. As a result, size of surface area and pore volume of ZCF had higher than ZBG whereas the pore size of ZBG had larger than ZCF. The previous studies reported that zeolite A materials exhibited the high surface area and pore volume with a small pore size resulted to the high adsorption capability [58,59], so it was possible that ZCF was higher lead adsorption than ZBG. For STD, size of surface area, pore volume, and pore size were 10.460 m^2/g, 0.030 cc/g, and 49.020 Å, respectively. As a result, size of surface area and pore volume of ZCF represented closely to STD whereas ZBG had less than STD. While pore size of ZBG was larger than ZCF and STD. Therefore, ZCF had the physiochemical properties similarly to STD more than ZBG corresponded to FESEM-FIB micrographs of ZCF similarly to STD. For pore size classification by the International Union of Pure and Applied Chemistry (IUPAC), the pore size of microporous, mesoporous, and macroporous were <20 Å, 20-500 Å, >500 Å, respectively [60], so the pore size of BFA, BFAH, ZBG,CFA, ZCF and STD were mesoporous whereas CFAA was microporous.

In Table 3, the chemical properties in chemical composition were determined in the mass percentage by weight (%wt). SiO_2, Al_2O_3, Fe_2O_3 and CaO were four main chemical properties in all samples. For BFA and BFAH, %wt of SiO_2 and Al_2O_3 were increased whereas Fe_2O_3 and CaO were decreased after the pretreatment process which might result in increasing of silicon and aluminum from removing other contaminant compounds in a raw material [52,61]. For CFA and CFAA, %wt of SiO_2 and Fe_2O_3 were increased whereas Al_2O_3 and CaO were decreased after the pretreatment process which might result from the acid washing method promoted the increasing of SiO_2 and dealuminated of Al_2O_3 [62]. In addition, the deceasing of CaO was a good advantage for zeolite A synthesis because CaO might interfere or inhibit the zeolite crystal nucleation in the synthesis process, and the reducing of CaO also helped to preserve the essential chemical elements for zeolite A synthesis [55].

3.1.3. XRD analysis

The XRD diffraction patterns of ZBG and ZCF were demonstrated in Figure 3a-c with comparing to STD. ZBG and ZCF illustrated the crystalline phases at 2θ of 7.2, 10.3, 12.6, 16.2, 21.8, 24, 26.2, 27.2, 30, 30.9, 31.1, 32.6, and 33.4 which represented the specific peaks of zeolite A characteristic. The results were correctly matched to the crystalline phases of STD and zeolite A standard pattern of JCPDS 39-222 [63] which confirmed that ZBG and ZCF were zeolite A [64].

3.1.4. FESEM-FIB analysis

FESEM-FIB micrographs of raw materials (BFA and CFA), raw materials with pretreatment (BFAH and CFAA), synthesized zeolite A adsorbents (ZBG and ZCF), and zeolite A standard (STD) demonstrated in Figure 4a-g. For raw materials, BFA was an irregular and rough surface shown in Figure 4a agreed to Zhang et al, 2020 which reported an irregular surface of prismatic, or fibrous with different sizes in the sugarcane bagasse ash (SCBA) [65] while CFA was a spherical shape and smooth surface shown in Figure 4b which was similarly found in other articles [66,67] at magnification of 1,500X with 50 μm. After pretreatment of raw materials, BFAH was also an irregular and rough surface shown in Figure 4c whereas CFAA was an evidently spherical shape and clearly other particle on surface area shown in Figure 4d at magnification of 1,500X with 50 μm because of impurities removed by an acid pretreatment process [68]. ZBG and ZCF represented the cubic shapes shown in Figure 4e-f at magnification 800X with 100 μm which were matched to the specific shape of zeolite A similarly to STD in Figure 4g at magnification 800X with 100 μm [68]. However, ZBG was more cubic shape and large crystallite size than ZCF which might cause from the different of zeolite synthesis method, temperature, and aging time for crystallization which they might affect to crystallite size of synthesized zeolite A [69]. ZBG used long aging time and low temperature which were better conditions to nucleate metastable phases of crystallization resulted to clear cubic shape with large crystallite size whereas ZCF used short aging time and high temperature resulted to less cubic shape with small crystallite size [69, 70, 71]. Moreover, a raw material might be another factor for zeolite A synthesis because the high silica source of raw material affects to good zeolite crystallite size [72,73] corresponded to XRF results that BFA had higher silica element than CFA.

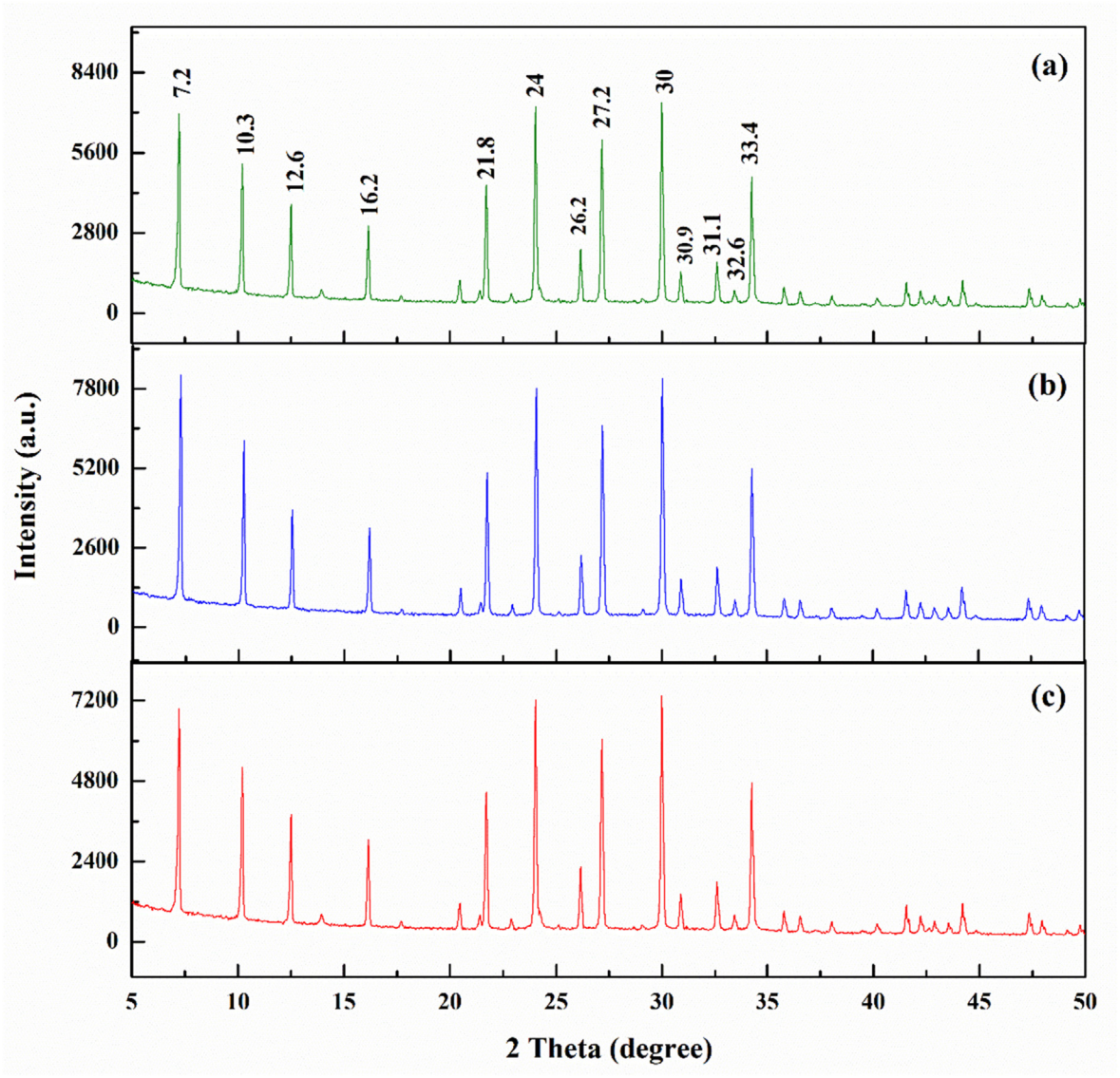

Figure 3. XRD diffraction patterns of (a) ZBG, (b) ZCF, and (c) STD.

3.1.5. XRF analysis

The chemical compositions of raw materials (BFA and CFA), raw materials with pretreatment (BFAH and CFAA), synthesized zeolite A adsorbents (ZBG and ZCF), and zeolite A standard (STD) were reported in Table 4. Six main chemical elements which were silicon (Si), aluminum (Al), iron (Fe), potassium (K), calcium (Ca), and phosphorus (P) were found in all materials, and Si was the highest mass in weight percentage (%wt). The mass percentages of Si in BFAH and CFAA were increased after the pretreatment process, so the pretreatment step is a necessary process to eliminate contaminated elements in order to increasing the mass of Si for zeolite synthesis. Especially, the acid wash treatment of CFA promoted highly increasing of Si and might affect to the changing of surface structure of fly ash. The acid solution caused a spherical smooth surface of fly ash to be a rough surface resulted in the increasing of the surface area of fly ash, and helped to enhance the quantity of Si source dissolved from fly ash for a good zeolite A synthesis [43]. The ratios of Si/Al of ZBG and ZCF were approximately 1.48 and 1.87 which ZBG was close to STD of 1.37 than ZCF. The theorical ratio of Si/Al of zeolite A should be equal to 1 [74]; however, the synthetic zeolite A might not meet this point because of the effects of various synthetic methods and the purity of silicon forms [94,95]. Not only ZBG and ZCF did not come to this perfect ratio of Si/Al but also the commercial zeolite A (STD). As a result, the ratio of Si/Al of ZBG and ZCF could be acceptance as zeolite A in a low silica-zeolite [77].

3.1.6. FTIR analysis

The chemical functional groups of ZBG, ZCF and STD were analyzed by FTIR, and their results demonstrated in Figure 5a-c. The main functional groups of ZBG and ZCF shown in Figure 5a-b were observed through the internal vibration of (Si, Al)–O asymmetric stretching at 1002.5 and 1000 cm^{-1}, the H_2O at 1666 and 1633 cm^{-1}, and OH (hydroxyl group) at 3455.6 and 3452 cm^{-1}, respectively. Moreover, the internal vibration of (Si, Al)–O bending, the external vibration of double four-rings (D_4R) and the internal vibration of (Si, Al)–O symmetric stretching were found at 463, 554, and 667 cm^{-1} of ZBG and 464.1, 553.6, and 668.3 cm^{-1} of ZCF, respectively which was closely main chemical functional groups of STD shown in Figure 5c and corresponded to the specific characteristic of zeolite A [78,79]. The specific characteristic of zeolite A was the internal vibration of (Si, Al)–O asymmetric stretching expresses in the frequency from 1091 to 1001 cm^{-1}, and the band at 567.4 cm^{-1} showed the external vibration of double four rings (D_4R) [80] similarly reported by other studies [79]. Normally, D_4R peak represents the occurrence of zeolite A, and is also an evidence for cubic prism structure in synthesized materials corresponding to specific zeolite

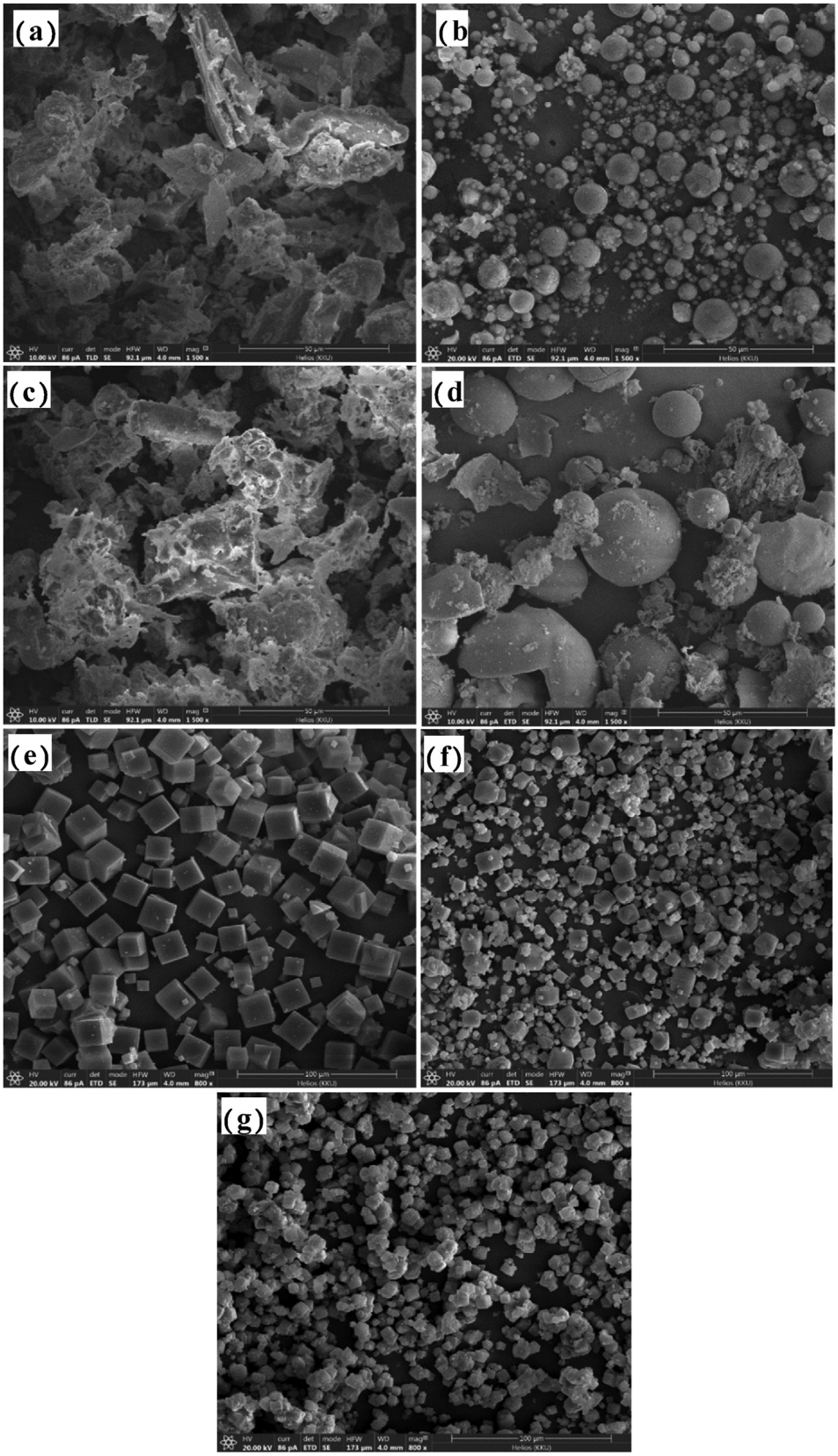

Figure 4. FESEM-FIB micrographs of (a) BFA, (b) CFA, (c) BFAH, (d) CFAA, (e) ZBG, (f) ZCF, and (g) STD.

Table 4. Chemical components of BFA, BFAH, ZBG, CFA, CFAA, ZCF, and STD by WD-XRF analysis.

No	Element	The percentage by weight (wt %)						
		BFA	BFAH	ZBG	CFA	CFAA	ZCF	STD
1	Si	61.60	64.10	51.00	15.20	55.40	56.30	47.00
2	Al	7.62	7.87	34.50	8.95	5.05	30.10	34.40
3	Fe	10.10	9.38	0.19	21.00	28.90	0.29	0.04
4	K	7.68	7.13	1.71	2.41	2.90	1.65	0.18
5	Ca	6.13	5.64	0.19	40.00	3.34	0.21	0.13
6	P	1.74	1.69	0.20	0.26	0.10	0.11	0.13
7	Mg	1.29	1.32	0.21	1.64	1.54	-	0.26
8	S	1.26	0.99	0.03	7.07	0.47	-	0.02
9	Ti	1.07	0.88	-	0.44	0.36	-	-
10	Mn	0.59	0.56	0.12	0.29	0.13	-	-
11	Cl	0.42	0.19	-	-	-	0.07	-
12	Ba	0.21	-	-	0.38	1.54	-	-
13	Zn	0.08	0.07	-	0.03	0.03	0.01	-
14	Sr	0.05	0.05	-	0.32	0.10	-	-
15	Cr	0.03	0.03	-	-	-	-	-
16	Cu	0.03	0.03	-	0.01	-	-	-
17	Rb	0.03	-	-	0.03	0.05	-	-
18	Ni	-	0.02	0.02	0.02	0.03	-	-
19	Na	-	-	11.70	1.80	-	11.10	17.80
20	Pd	-	-	0.19	-	-	0.10	0.11
21	As	-	-	-	0.06	-	-	-
22	Zr	-	-	-	0.03	0.09	0.01	0.01
Total		100	100	100	100	100	100	100

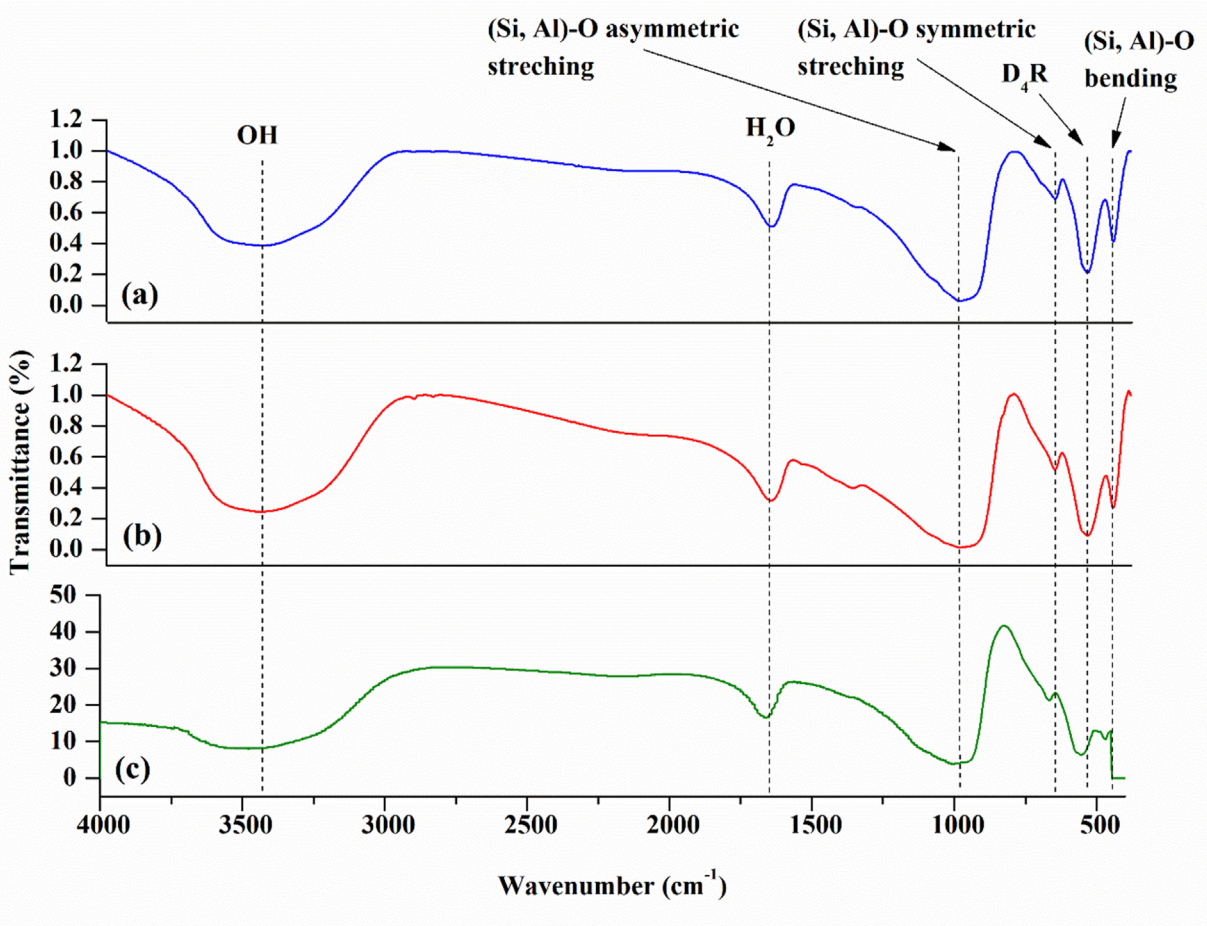

Figure 5. Chemical functional groups of (a) ZBG, (b) ZCF, and (c) STD.

A structure [80]. Moreover, the structure of zeolite A is also confirmed by a β-cage which is the basic structure interconnected with D_4R [56]. In addition, the band at 485.8 cm^{-1} was related to the internal vibration of (Si, Al)–O bending.

3.2. Batch adsorption studies

3.2.1. The effect of dosage

The adsorbent dosages of ZBG and ZCF from 0.005 g to 0.035 g were investigated for the influence of the amount of adsorbent on lead removal efficiencies of ZBG and ZCF shown in Figure 6a. The highest lead removal efficiencies of ZBG and ZCF of 100% were found at 0.02 g. Lead removal efficiencies were increased with the increasing of the adsorbent dosage from 0.005 g to 0.035 g because the negatively charged exchange sites were incremented corresponding to the increasing of adsorbent dosage [81]. However, the adsorbent dosages were higher than 0.02 g demonstrated constant lead removal efficiencies of 100%. Therefore, the optimum adsorbent dosages of ZBF and ZCF were 0.02 g and were used to study the effect of contact time.

3.2.2. The effect of contact time

The contact time of ZBG and ZCF from 1 h to 5 h were selected to investigate the optimum contact time on lead removal efficiencies of ZBG and ZCF shown in Figure 6b. ZBG showed the highest lead removal efficiency of 100 % for 2 h whereas ZCF showed the highest lead removal efficiency of 100 % for 1 h. Lead removal efficiencies of both zeolite A adsorbents were increased with the increasing of contact time from 1 to 5 h; however, lead removal efficiencies were constant after 2 h for ZBG and 1h for ZCF. Therefore, the conditions of ZBG and ZCF were 0.02 g for 2 h and 0.02 g for 1 h, respectively which they were used for the effect of pH.

3.2.3. The effect of pH

The effects of pH at 1, 3, 5, 7, 9, and 11 of ZBG and ZCF were investigated the optimum pH on lead removal efficiencies shown in Figure 6c. ZBG showed the highest lead removal efficiencies of 100 % in pH range of 5–9 whereas ZCF showed the highest lead removal efficiencies of 100 % in pH range of 5–11. The results were similar pH range for lead adsorption reported by other studies [36,82]. As a result, both zeolite adsorbents could be applied for lead adsorption in wastewater with various pH conditions of acid, neutral, and base. However, pH 5 was preferred because hydroxyl groups of zeolites (Si–OH and Al–OH) can be ionized and adsorbed lead in the water with weak acid condition [83], and other previous studies also reported pH of 5 was appropriate for lead adsorption in wastewater [50,84]. This result also matched to the point of zero charge (pH_{pzc}) of zeolite A on metal (II) ions of other studies at pH of 5.4 [85,86]. Moreover, the solution at pH < 3 was strong acid and highly hydrogen ions (H^+) combined with zeolite A better than lead ions (Pb^{2+}), thus it might create the competition between H^+ and Pb^{2+} onto the zeolite A adsorption [87]. For pH > 3, H^+ decreased meant the increasing of Pb^{2+} adsorption by the negatively charged sites on the zeolite A [88]. Therefore, the optimum pH of ZBG and ZCF was pH 5, and the optimum conditions of ZBG and ZCF were 0.02 g, 2 h, pH 5 and 0.02

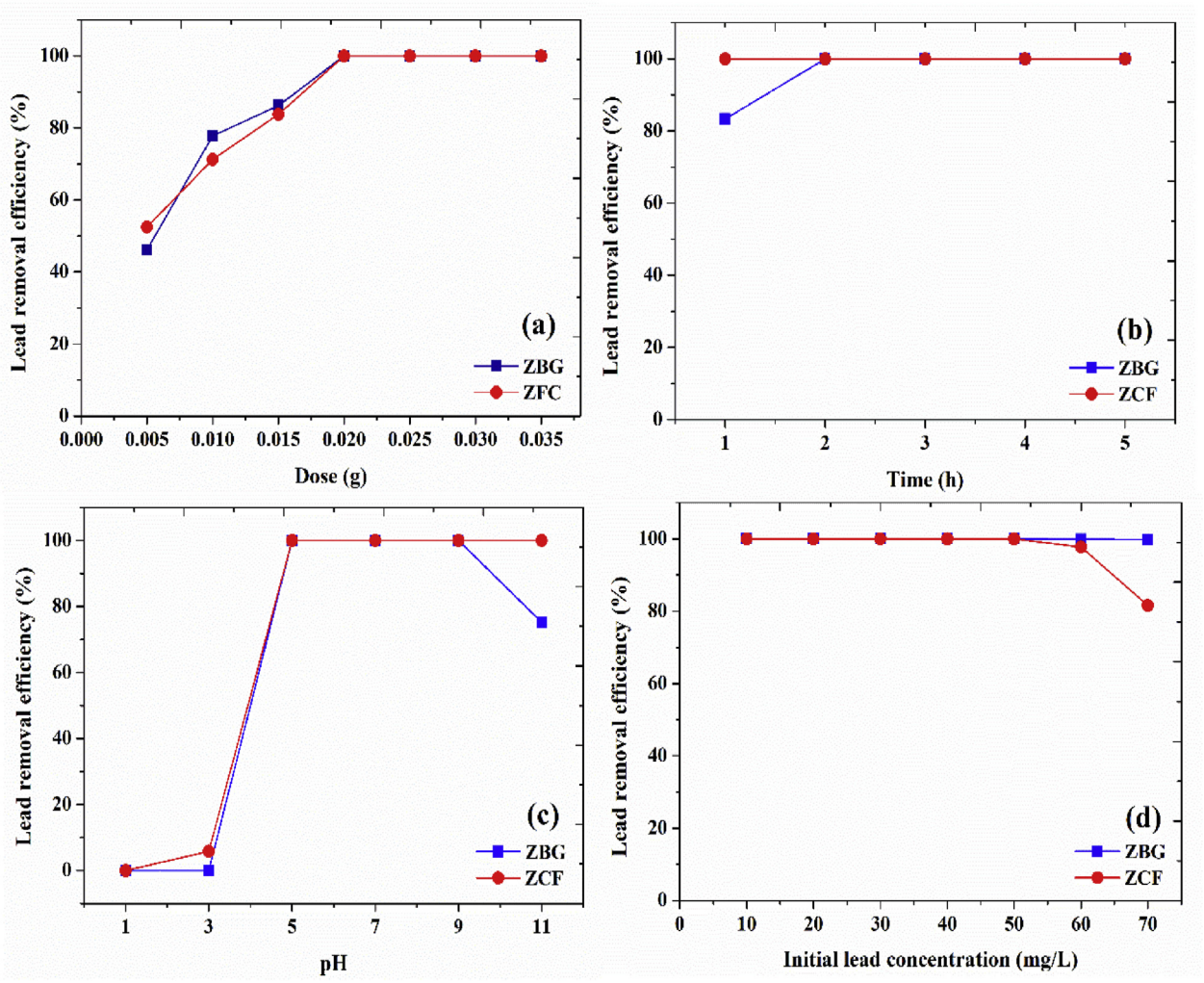

Figure 6. The batch adsorption studies of ZBG and ZCF (a) effect of dose, (b) effect of contact time, (c) effect of pH, and (d) effect of initial lead concentration.

g, 1 h, pH 5, respectively which they were used for the effect of initial lead concentration.

3.2.4. The effect of initial lead concentration

The effect of initial concentration from 10 mg/L to 70 mg/L of ZBG and ZCF were investigated the influence of concentration on lead removal efficiencies showed in Figure 6d. ZBG represented the lead removal efficiencies of 100% for all concentrations while ZCF represented the lead removal efficiencies of 100% for the concentrations from 10 mg/L to 50 mg/L. Therefore, ZBG and ZCF were possible applied for lead removal in wastewater.

3.3. Zeta potential analysis

The surface charge of adsorbents might help to describe the ability of lead adsorptions of ZBG and ZCF, so the zeta potential studies were conducted with various pH values. Figure 7 demonstrated the results of the zeta potential analysis of ZBG, ZCF, and STD which they were separated to 3 zones, and all zeolite A adsorbents represented the same tend. For zone I, the zeta potential values of ZBG, ZCF and STD were loss of adsorption at pH < 3 because of an overabundance of protons resulted to inhibit lead absorptions with severe competition between hydrogen (H^+) and lead ions (Pb^{2+}), and the surface charges of ZBG and ZCF were positively charged in this zone. For zone II, the surface charges of all zeolite A adsorbents represented negatively charged at pH values of 3–9 due to the dissociation of the hydroxyl groups (OH^-) which zeolite surfaces were easily de-protonated to a form of Si–O throughout a wide pH range and led to more negatively charged on the surface [89]. Moreover, the negatively charged had a greater coordinative affinity towards lead cations by the electrostatic forces of attraction to capture lead ions via surface complexation resulting in the formation of chelate complexes of lead adsorption [90]. However, pH 5 demonstrated the highest negatively charged in all zeolite A adsorbents which agreed to the result of effect of pH that pH 5 demonstrated the highest lead removal efficiencies of ZBG and ZCF. For zone III, all zeolite A adsorbents represented the reduction of the negative charged at pH > 9 which they lead adsorptions of zeolite A adsorbents might be decreased.

3.4. Adsorption isotherms

Figure 8a-d demonstrated the adsorption isotherms studies of ZBG and ZCF with plotting of Langmuir and Freundlich models, and the adsorption parameters were reported in Table 5.

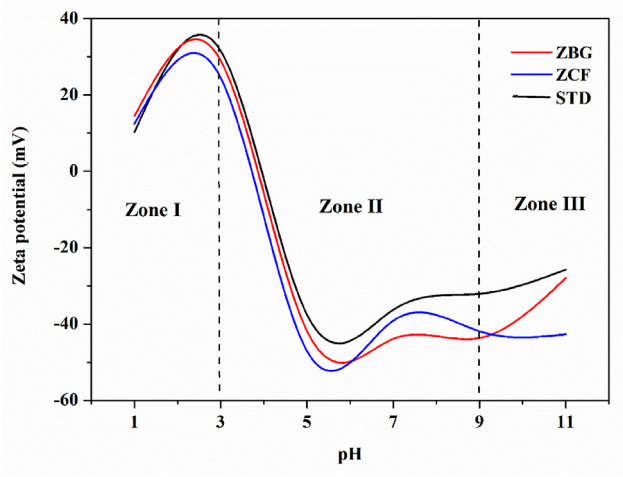

Figure 7. The zeta potential analysis of ZBG, ZCF, and STD in various pH solutions.

For Langmuir model, the maximum adsorption capacities (q_m) of ZBG and ZCF were 625 and 556 mg/g, respectively which ZBG had higher maximum adsorption capacity than ZCF. Moreover, Langmuir adsorption constants (b) of ZBG and ZCF were 0.036 and 0.015, respectively. For Freundlich model, the constant depicting of the adsorption intensity (1/n) is an important parameter to explain how the lead concentration were adsorbed by ZBG and ZCF ($1/n$) of ZBG and ZCF were 0.135 and 0.074, respectively, and they were assigned to pseudo-irreversible adsorption of ZCF for $1/n < 0.1$ and favorable adsorption for $0.1 < 1/n < 0.5$ by Tseng, Ru-Ling and wu, Feng-Chin, 2008 [91]. Freundlich adsorption constants (K_F) were 902.820 mg/g and 515.470 mg/g for ZBG and ZCF, respectively. Generally, the fitting isotherm model is decided by higher R^2, so the adsorption isotherms of ZBG and ZCF were well explained by Langmuir model with higher R^2 than Freundlich model, and the adsorption patterns of both zeolite A adsorbents were explained by the physical adsorption process similarly to adsorption pattern reported by Liu et al., 2016 [92] and Rondón et al., 2013 [35]. Moreover, the maximum adsorption capacities (q_m) of ZBG and ZCF were higher than other studies reported in Table 6.

3.5. Adsorption kinetics

The adsorption kinetic is an important study to explain an adsorption mechanism including rate of adsorption to time by adsorbent [94]. The adsorption kinetics of ZBG and ZCF were plotted following to a pseudo-first-order kinetic model (PFO) and a pseudo-second-order kinetic model (PSO) shown in Figure 9a-d, and the adsorption equilibrium of lead removal on ZBG and ZCF represented in Figure 9e-f. Moreover, the kinetic parameters were reported in Table 7.

In Table 7, the adsorption kinetics of ZBG and ZCF were corresponded PSO at R^2 equal to 1and 0.995, respectively. The adsorption capacities of ZBG and ZCF were 500 and 454.55 mg/g, respectively, and k_2 of ZBG and ZCF were 0.00015 and 0.00020 g/mg min, respectively. As a result, ZBG demonstrated higher lead adsorption capacity with a little lower adsorption constant rate than ZCF. Therefore, the adsorption mechanisms of both zeolite A adsorbents involved chemisorption with relating to physiochemical interaction [95]. In Table 8, this study was similar adsorption mechanism to other studies, and the maximum adsorption capacities (q_m) of ZBG and ZCF were higher than all other studies. Finally, the adsorption equilibriums of ZBG and ZCF were demonstrated in Figure 8e-f, and the rates of lead adsorption of ZBG and ZCF were 10 min and 80 min, respectively. Therfore, ZBG represented the higher rate of lead adsorption with fast kinetic reaction than ZCF.

3.6. The possible mechanism of lead adsorptions on ZBG and ZCF

The possible mechanism of lead adsorptions on ZBG and ZCF modified from X. Fan et al, 2021 [101] demonstrated in Figure 10. The oxygen (O) skeleton in silica and alumina tetrahedron structures of zeolite A is a negatively charged. Lead ions are acidic and can accept electrons following to Lewis acid-base theory [101], so O in the zeolite A structure can create coordination with lead ions. The greater electronegativity of the lead ions is more easily to attract electron clouds of negatively charged oxygen, and the stronger coordinate bonds establish with O. Furthermore, the ionization and hydrolysis processes show silanol (≡Si–OH) and aluminols (≡Al–OH) sites on the surface of zeolite A [83, 102]. Therefore, the surface of ZBG and ZCF might be found alumino silicates of lead complexes or other coordination compounds after lead adsorption [103]. In addition, zeolite A might have an ion-exchange property for heavy metal adsorptions [104,105].

3.7. The economic view for the application of zeolite A adsorbents

BFA is a solid waste from sugar mills that includes a significant quantity of unburned carbon and potential harm to humans, plants, and animals via the air, water, and soil [106]. Moreover, bagasse fly ash is

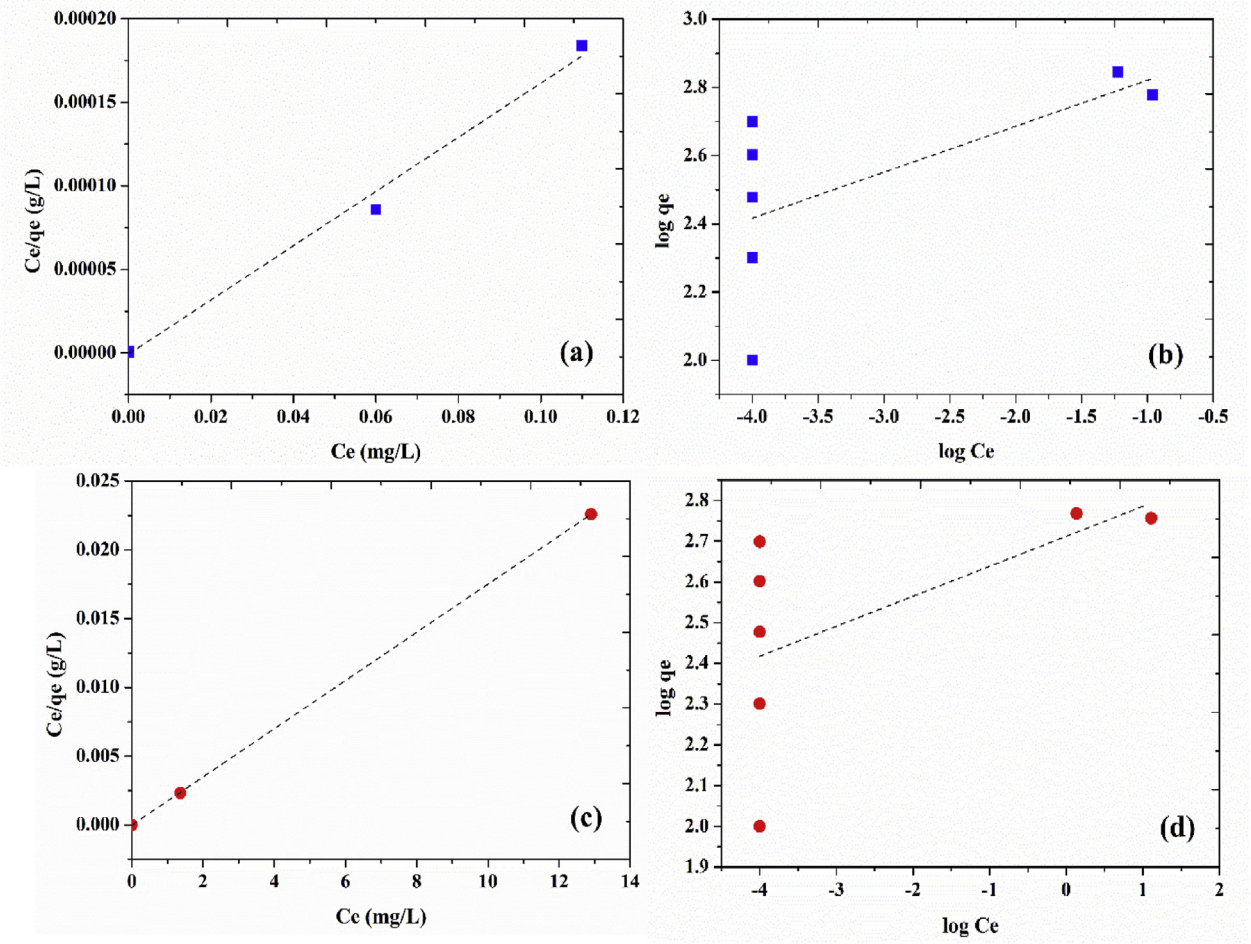

Figure 8. Adsorption isotherms of (a) Langmuir and (b) Freundlich isotherm models for lead adsorptions on ZBG (c) Langmuir and (d) Freundlich isotherm models for lead adsorptions on ZCF.

Table 5. Langmuir and Freundlich isotherm parameters for lead adsorptions on ZBG and ZCF.

Sample	Langmuir constants			Freundlich constants		
	q_m (mg/g)	b (L/mg)	R^2	K_F (mg/g)	$1/n$	R^2
ZBG	625	0.036	0.995	902.820	0.135	0.415
ZCF	556	0.015	1	515.470	0.074	0.353

extremely tiny particle sizes and lightweight, so it is easily airborne and contributes to air pollution and respiratory issues of human [107]. Generally, BFA is disposed in landfill, and the increasing of BFA creates the waste management problem with finding new landfills. For CFA, it is a solid waste produced by power stations which approximately 500 million tons per year of fly ash are globally discharged [108]. Due to its fine structure and hazardous ingredients, coal fly ash continuously represents the growing threat to the environment. Moreover, due to the enormous amount of coal combustion waste produced in comparison to use, the disposal facilities running out of storage capacity is not enough for a landfill. As a result, the new waste management of BFA and CFA is an interesting option especially recycled them for other purpose for reducing waste volumes.

The recycling of wastes is one of sustainable development based on the circular economy which directly corresponds to economic and technological justification in 5 R principles of reduce, replacement, recovery, reuse and recycling [109]. Therefore, uses of BFA and CFA as affordable raw materials for synthesis of zeolite A adsorbents for lead removal in wastewater are an interesting choice to obtain two benefits of waste management and water quality. In addition, the recycle of these wastes might increase waste value in the economic point.

Table 6. Comparison of Langmuir and Freundlich isotherm parameters for lead adsorption on zeolite adsorbents.

Raw material	Type of zeolite	Langmuir constants			Freundlich constants			Reference
		q_m (mg/g)	b (L/mg)	R^2	K_F (mg/g)	$1/n$	R^2	
CFA	K	98	0.24	0.987	1.51	0.30	0.997	[46]
BFA	P	73.63	0.16	0.582	34.02	0.14	0.898	[93]
CFA	NaX	142.86	0.30	0.998	47.86	0.23	0.845	[92]
Kaolin	A	14.64	5.42	0.999	11.34	7.69	0.710	[35]
ZBG	A	625	0.036	0.995	902.820	0.135	0.415	This study
ZCF	A	556	0.015	1	515.470	0.074	0.353	This study

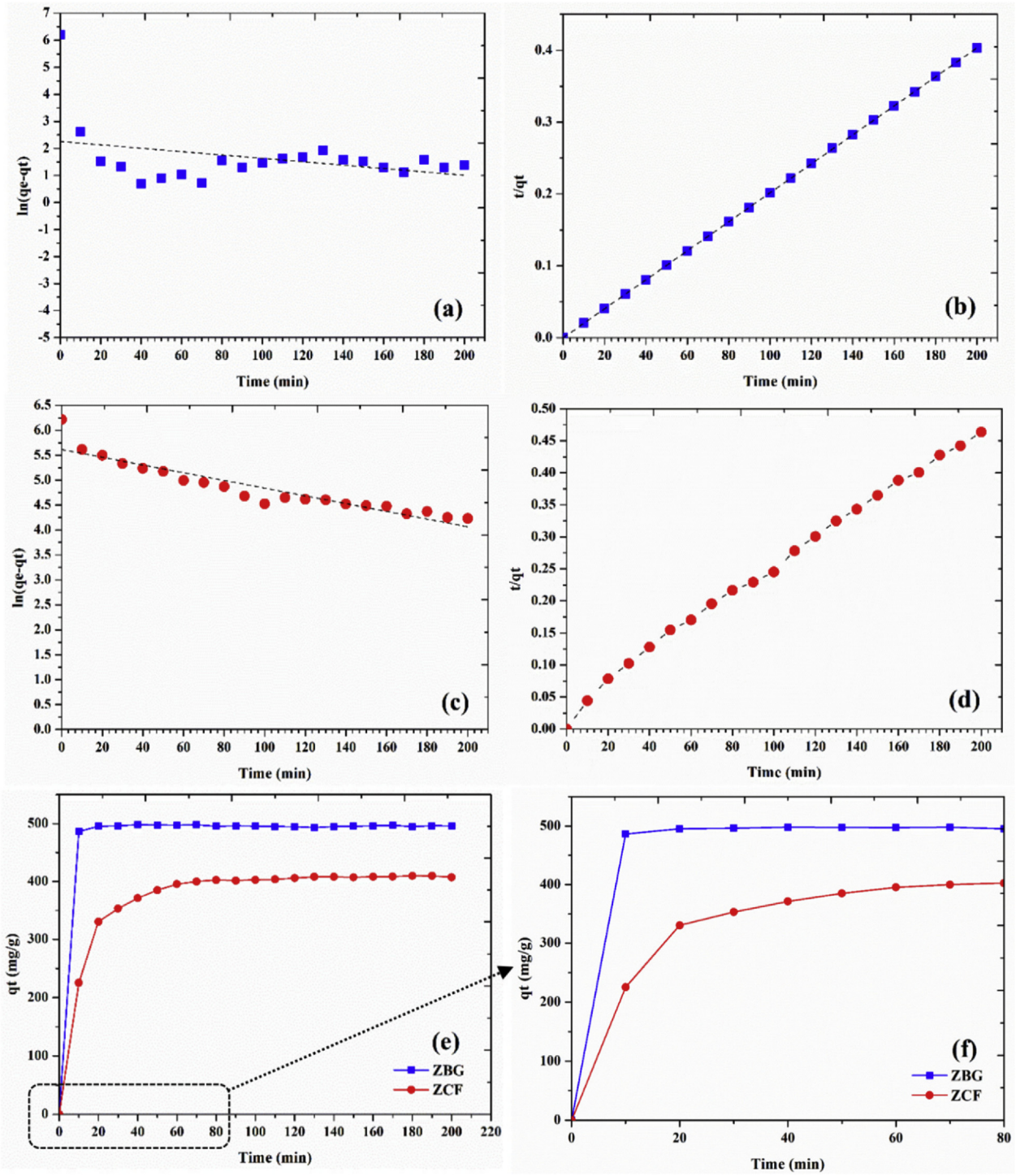

Figure 9. Kinetic models of (a) pseudo-first-order kinetic model (b) pseudo-second-order kinetic model for lead adsorptions on ZBG (c) pseudo-first-order kinetic model (d) pseudo-second-order kinetic model for lead adsorptions on ZCF, and adsorption equilibrium of lead removals on ZBG and ZCF in a range of (e) 0-220 min, and (f) 0-80 min.

Table 7. Kinetic parameters for lead adsorptions on ZBG and ZCF.

Sample	Pseudo-first-order kinetic model			Pseudo-second-order kinetic model		
	q_e (mg/g)	k_1 (1/min.)	R^2	q_e (mg/g)	k_2 (g/mg min)	R^2
ZBG	9.563	0.0062	0.118	500	0.00015	1
ZCF	274.293	0.0077	0.872	454.55	0.00020	0.995

For ZBG, 20 g of BFA got about 17 g of BFAH, and 15 g of BFAH obtained approximately 8 g of ZBG. If the sugarcane factory has 1 ton of BFA wastes per year, it can produce approximately 400 kg of ZBG. If the price of commercial zeolite A (AR grade) is about 4,000 THB/100g, 400 kg of ZBG is equal to 1.6 million THB. Then, this benefit value is reduced by the cost of zeolite synthesis proximately a half of selling price. Finally, the net profit is about 800,000 THB per year. For ZCF, 90 g of CFA got about 9 g of CFAA, and 9 g of CFAA obtained approximately 5 g of ZCF. If the power plant has 1 ton of BFA wastes per year, it can produce

Table 8. Comparison of pseudo-first order and pseudo-second order of kinetic parameters for lead adsorptions on adsorbents.

Adsorbent	Pseudo-first-order kinetic model			Pseudo-second-order kinetic model			Reference
	q_e (mg/g)	k_1 (1/min)	R^2	q_e (mg/g)	k_2 (g/mg min)	R^2	
Natural zeolite	23.30	2.22	0.999	23.30	0.43	1	[96]
Zeolite (Faujasite and Zancrinite)	14.87	0.31	0.997	15.83	0.04	0.999	[97]
BFA	17.75	1.07×10^{-2}	0.952	33.83	1.31×10^{-3}	0.999	[93]
CFA	48.54	1.24	0.826	50.23	0.04	0.999	[98]
CFA (Faujasite)	21.04	20.54×10^{-3}	0.918	75.76	13.5×10^{-4}	0.999	[92]
Linde F(K) zeolite	3.16	0.004	0.956	46.51	0.05	0.997	[90]
Clinoptilolite (Modified zeolite)	19.86	0.03	0.884	49.50	1.63×10^{-3}	0.991	[99]
Clinoptilolite modified with NZVI (zeolite A)	123.10	0.29	0.953	137.90	3.561×10^{-3}	0.977	[100]
ZBG	9.563	0.0062	0.118	500	0.00015	1	This study
ZCF	274.293	0.0077	0.872	454.55	0.00020	0.995	This study

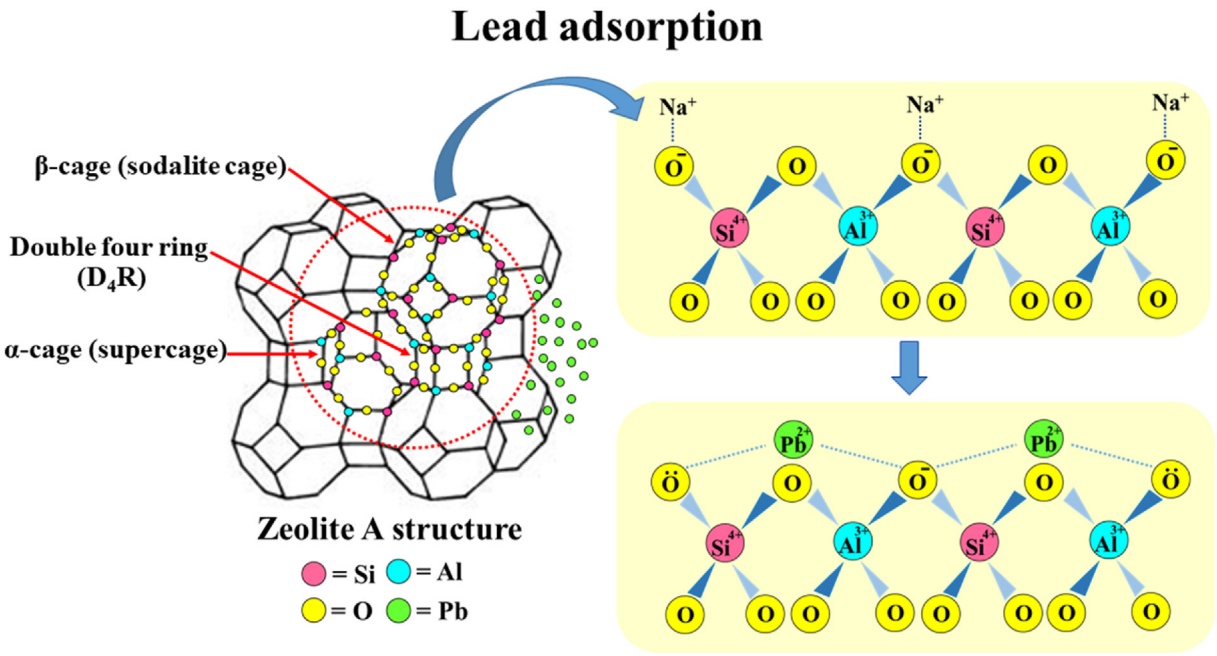

Figure 10. The possible mechanism of lead adsorptions on ZBG and ZCF.

approximately 56 kg of ZCF. If the price of commercial zeolite A (AR grade) is about 4,000 THB/100g, 56 kg of ZBG is equal to 224,000 THB. Then, this benefit value is reduced by the cost of zeolite synthesis proximately a half of selling price. Finally, the net profit is about 112,000 THB per year. Therefore, the recycling of BFA and CFA are one of sustainable solid waste management, and ZBG and ZCF are potential adsorbents for lead adsorptions as inexpensive adsorbents for the wastewater treatment in the future.

4. Conclusions

The present study was successfully synthesized zeolite A adsorbents from bagasse fly ash (BFA) and coal fly ash (CFA). The method modifications for zeolite A synthesis were suitable to raw materials from industrial wastes (BFA and CFA), so the specific characteristics of synthesized zeolite A adsorbents were close to zeolite A standard (STD) through various characterization techniques. For a series of batch experiments, both zeolite A adsorbents demonstrated high lead removal efficiencies of 100% with the optimum conditions of 0.02 g, 2 h, pH 5, 10-70 mg/L of lead concentrations for ZBG, and 0.02 g, 1 h, pH 5, 10-50 mg/L of lead concentrations for ZCF. The zeta potential studies of ZBG and ZCF were the highest negatively charged at pH 5 corresponded to the highest lead adsorption of both zeolite A adsorbents at pH of 5. For adsorption isotherms, ZBG and ZCF were corresponded to Langmuir isotherm which correlated to the physical adsorption process at R^2 of 0.995 and 1, respectively. For adsorption kinetics, ZBG and ZCF were corresponded a pseudo-second-order kinetic model which correlated to the physiochemical interaction at R^2 of 1 and 0.995, respectively. As a result, this study achieved two purposes of waste management by use of industrial waste recycling as low-cost adsorbents and improving of water quality by applying for lead removals in wastewater. Therefore, ZBG and ZCF are high potential zeolite A adsorbents to apply for lead removal in real industrial wastewater in future. In the future work, the continuous flow system, adsorbent regeneration, and competing other ions for real.

Declarations

Author contribution statement

Sirirat Jangkorn: Performed the experiments; Analyzed and interpreted the data; Wrote the paper.

Sujittra Youngme: Analyzed and interpreted the data; Wrote the paper.

Pornsawai Praipipat: Conceived and designed the experiments; Performed the experiments; Analyzed and interpreted the data; Contributed reagents, materials, analysis tools or data; Wrote the paper.

Funding statement

This work was supported by Loei Rajabhat University, Thailand; The Office of the Higher Education Commission and The Thailand Research Fund grant (MRG6080114), Thailand; Coordinating Center for Thai Government Science and Technology Scholarship Students (CSTS) and National Science and Technology Development Agency (NSTDA) Fund grant (SCHNR2016-122), Thailand; and Research and Technology Transfer Affairs of Khon Kaen University, Thailand.

Data availability statement

Data will be made available on request.

Declaration of interests statement

The authors declare no conflict of interest.

Additional information

No additional information is available for this paper.

References

[1] H. Ali, E. Khan, I. Ilahi, Environmental chemistry and ecotoxicology of hazardous heavy metals: environmental persistence, toxicity, and bioaccumulation, J. Chem. 2019 (2019) 1–14.
[2] F. Length, Heavy metal pollution and human biotoxic effects, Phys. Sci. Int. J. 2 (2007) 112–118.
[3] R. Naseem, S.S. Tahir, Removal of Pb (II) from aqueous/acidic solutions by using bentonite as an adsorbent, Water Res 35 (2001) 3982–3986.
[4] Q. Mahmood, A. Rashid, S.S. Ahmad, M.R. Azim, M. Bilal, Current Status of Toxic Metals Addition to Environment and its Consequences, Environmental Pollution, 2012, pp. 35–69.
[5] M.D. Meitei, M.N.V. Prasad, Lead (II) and cadmium (II) biosorption on Spirodela polyrhiza (L.) schleiden biomass, J. Environ. Chem. Eng. 1 (2013) 200–207.
[6] O. Abollino, M. Aceto, M. Malandrino, C. Sarzanini, E. Mentasti, Adsorption of heavy metals on Na-montmorillonite. Effect of pH and organic substances, Water Res 37 (2003) 1619–1627.
[7] F. Fu, Q. Wang, Removal of heavy metal ions from wastewaters: a review, J. Environ. Manage. 92 (2011) 407–418.
[8] M.A. Barakat, New trends in removing heavy metals from industrial wastewater, Arab. J. Chem. 4 (2011) 361–377.
[9] M. Minceva, L. Markovska, V. Meshko, Removal of Zn^{2+}, Cd^{2+} and Pb^{2+} from binary aqueous solution by natural zeolite and granulated activated carbon, Maced. J. Chem. Chem. Eng. 26 (2007) 125–134.
[10] H. Sadegh, M. Mazloumbilandi, M. Chahardouri, Low-cost Materials with Adsorption Performance 2017, Springer International Publishing AG, 2019.
[11] R. Cheerarot, C. Jaturapitakkul, A study of disposed fly ash from landfill to replace Portland cement, Waste Manag 24 (2004) 701–709.
[12] G.C. Cordeiro, R.D.T. Filho, E.M.R. Fairbairn, L.M.M. Tavares, C.H. Oliveira, Influence of mechanical grinding on the pozzolanic activity of residual sugarcane bagasse ash, in: International RILEM Conference on Use of Recycled Materials in Building and Structures, 2004, pp. 731–740.
[13] P. Thuadaij, A. Nuntiya, Preparation and characterization of faujasite using fly ash and amorphous silica from rice husk ash, Procedia Eng 32 (2012) 1026–1032.
[14] S. Kuroki, T. Hashishin, T. Morikawa, K. Yamashita, M. Matsuda, Selective synthesis of zeolites A and X from two industrial wastes: crushed stone powder and aluminum ash, J. Environ. Manage. 231 (2019) 749–756.
[15] W. Tariq, M. Saifullah, T. Anjum, M. Javed, N. Tayyab, I. Shoukat, Removal of heavy metals from chemical industrial wastewater using agro based bio-sorbents removal of heavy metals from chemical industrial wastewater using agro based bio-sorbents, ACMY 2 (2019) 9–14.
[16] N.A. Rosli, M.H. Zawawi, R.A. Bustami, F. Hipni, M.A. Kamruddin, Adsorption of lead using jackfruit peel activated carbon, Appl. Mech. Mater. 773–774 (2015) 1079–1084.
[17] C.-G. Lee, J.-W. Jeon, M.-J. Hwang, K.-H. Ahn, C. Park, J.-W. Choi, S.-H. Lee, Lead and copper removal from aqueous solutions using carbon foam derived from phenol resin, Chemosphere 130 (2015) 59–65.
[18] A.A. Alswat, M. Bin Ahmad, T.A. Saleh, Zeolite modified with copper oxide and iron oxide for lead and arsenic adsorption from aqueous solutions, J. Water Supply Res. T. 65 (2016) 465–479.
[19] A.A. Salunkhe, A. Mahajan, Analysis of absorbents and their application for lead removal, IJCIET 9 (2018) 1913–1919.
[20] M. Kragović, A. Daković, Ž. Sekulić, M. Trgo, M. Ugrina, J. Perić, G.D. Gatta, Removal of lead from aqueous solutions by using the natural and Fe(III)-modified zeolite, Appl. Surf. Sci. 258 (2012) 3667–3673.
[21] V.O. Njoku, A.A. Ayuk, E.E. Ejike, E.E. Oguzie, C.E. Duru, O.S. Bello, Cocoa pod husk as a low cost biosorbent for the removal of Pb (II) and Cu (II) from aqueous solutions, Aust. J. Basic & Appl. Sci. 5 (2011) 101–110.
[22] N. Shilawati Ehishan, N. Sapawe, Performance studies removal of chromium (Cr^{6+}) and lead (Pb^{2+}) by oil palm frond (OPF) adsorbent in aqueous solution, Mater. Today: Proc. 5 (2018) 21897–21904.
[23] C. Liu, H.H. Ngo, W. Guo, Watermelon rind: agro-waste or superior biosorbent, Appl. Biochem. Biotechnol. 167 (2012) 1699–1715.
[24] A. Dubey, S. Shiwani, Adsorption of lead using a new green material obtained from Portulaca plant, IJEST 9 (2012) 15–20.
[25] R.M. Taha, N.W. Haron, S.N. Wafa, Morphological and tissue culture studies of platycerium coronarium, a rare ornamental fern species from Malaysia, Am. Fern J. 101 (2011) 241–251.
[26] X. Hu, M. Zhao, G. Song, H. Huang, Modification of pineapple peel fibre with succinic anhydride for Cu^{2+}, Cd^{2+} and Pb^{2+} removal from aqueous solutions, Environ. Technol. 32 (2011) 739–746.
[27] O. Kaplan Ince, M. Ince, V. Yonten, A. Goksu, A food waste utilization study for removing lead (II) from drinks, Food Chem 214 (2017) 637–643.
[28] N.C. Feng, X.Y. Guo, Characterization of adsorptive capacity and mechanisms on adsorption of copper, lead and zinc by modified orange peel, T Nonferr. Metal. Soc. 22 (2012) 1224–1231.
[29] T. Wajima, Preparation of adsorbent with lead removal ability from paper sludge using sulfur-impregnation, APCBEE Procedia 10 (2014) 164–169.
[30] D.H. Huy, E. Seelen, V. Liem-Nguyen, Removal mechanisms of cadmium and lead ions in contaminated water by stainless steel slag obtained from scrap metal recycling, J. Water Process. Eng. 36 (2020) 101369.
[31] M. Martinez, N. Miralles, S. Hidalgo, N. Fio, I. Villaescusa, J. Poch, Removal of lead (II) and cadmium (II) from aqueous solutions using grape stalk waste, J. Hazard. Mater. 133 (2006) 203–211.
[32] V.K. Gupta, I. Ali, Removal of lead and chromium from wastewater using bagasse fly ash - a sugar industry waste, J. Colloid Interface Sci. 271 (2004) 321–328.
[33] A.D. Papandreou, C.J. Stournaras, D. Panias, I. Paspaliaris, Adsorption of Pb (II), Zn (II) and Cr (III) on coal fly ash porous pellets, Miner. Eng. 24 (2011) 1495–1501.
[34] H.S. Ibrahim, T.S. Jamil, E.Z. Hegazy, Application of zeolite prepared from Egyptian kaolin for the removal of heavy metals: II. Isotherm models, J. Hazard. Mater. 182 (2010) 842–847.
[35] W. Rondón, D. Freire, Z. de Benzo, A.B. Sifontes, Y. González, M. Valero, J.L. Brito, Application of 3A zeolite prepared from venezuelan kaolin for removal of Pb (II) from wastewater and its determination by flame atomic absorption spectrometry, Am. J. Anal. Chem. 4 (2013) 584–593.
[36] T.S. Jamil, H.S. Ibrahim, I.H. Abd El-Maksoud, S.T. El-Wakeel, Application of zeolite prepared from Egyptian kaolin for removal of heavy metals: I. Optimum conditions, Desalination 258 (2010) 34–40.
[37] T. Hussain, A.I. Hussain, S.A.S. Chatha, A. Ali, M. Rizwan, S. Ali, P. Ahamd, L. Wijaya, M.N. Alyemeni, Synthesis and characterization of Na-zeolites from textile waste ash and its application for removal of lead (Pb) from wastewater, Int. J. Environ. Res. Public Health. 18 (2021) 3373.
[38] A.M. Cardoso, M.B. Horn, L.S. Ferret, C.M.N. Azevedo, M. Pires, Integrated synthesis of zeolites 4A and Na-P1 using coal fly ash for application in the formulation of detergents and swine wastewater treatment, J. Hazard. Mater. 287 (2015) 69–77.
[39] J.A. Oliveira, F.A. Cunha, L.A.M. Ruotolo, Synthesis of zeolite from sugarcane bagasse fly ash and its application as a low-cost adsorbent to remove heavy metals, J. Clean. Prod. 229 (2019) 956–963.
[40] M. Łach, A. Grela, N. Komar, J. Mikuła, M. Hebda, Calcined post-production waste as materials suitable for the hydrothermal synthesis of zeolites, Mater 12 (2019) 2742.
[41] M.P. Moisés, C.T.P. da Silva, J.G. Meneguin, E.M. Girotto, E. Radovanovic, Synthesis of zeolite NaA from sugarcane bagasse ash, Mater. Lett. 108 (2013) 243–246.
[42] S.F. Ferrarini, A.M. Cardoso, A. Paprocki, M. Pires, Integrated synthesis of zeolites using coal fly ash: element distribution in the products, washing waters and effluent, J. Braz. Chem. Soc. 27 (2016) 2034–2045.
[43] C.-F. Wang, J.-S. Li, L.-J. Wang, X.-Y. Sun, Influence of NaOH concentrations on synthesis of pure-form zeolite A from fly ash using two-stage method, J. Hazard. Mater. 155 (2008) 58–64.
[44] N. Abdus-Salam, F.A. Adekola, The influence of pH and adsorbent concentration on adsorption of lead and zinc on a natural goethite, AJST 6 (2010) 55–66.
[45] C. Arunlertaree, W. Kaewsomboon, A. Kumsopa, P. Pokethitiyook, P. Panyawathanakit, Removal of lead from battery manufacturing wastewater by egg shell, Songklanakarin J. Sci. Technol. 29 (2007) 857–868.
[46] Y. Kobayashi, F. Ogata, C. Saenjum, T. Nakamura, N. Kawasaki, Removal of Pb^{2+} from aqueous solutions using K-type zeolite synthesized from coal fly ash, Water 12 (2020) 2375.
[47] J. Racyte, M. Rimeika, H. Bruning, pH effect on decolorization of raw textile wastewater polluted with reactive dyes by advanced oxidation with U/VH_2O_2, Environ. Prot. Eng. 35 (2009) 167–178.
[48] S.I. Mussatto, M. Fernandes, G.J.M. Rocha, J.J.M. Órfão, J.A. Teixeira, I.C. Roberto, Production, characterization and application of activated carbon from Brewer's spent grain lignin, Bioresour. Technol. 101 (2010) 2450–2457.

[49] E. Šabanović, M. Memić, J. Sulejmanović, A. Selović, Simultaneous adsorption of heavy metals from water by novel lemon-peel based biomaterial, Polish, J. Chem. Technol. 22 (2020) 46–53.

[50] A. Threepanich, P. Praipipat, Efficacy Study of Recycling Materials by Lemon Peels as Novel lead Adsorbents with Comparing of Material Form Effects and Possibility of Continuous Flow experiment, Environmental Science and Pollution Research, 2022.

[51] P. Bhunia, S. Chatterjee, P. Rudra, S. De, Chelating polyacrylonitrile beads for removal of lead and cadmium from wastewater, Sep. Purif. Technol. 193 (2018) 202–213.

[52] G.C. Cordeiro, T.R. Barroso, R.D. Toledo Filho, Enhancement the properties of sugar cane bagasse ash with high carbon content by a controlled re-calcination process, KSCE J. Civ. Eng. 22 (2018) 1250–1257.

[53] G.L. Fisher, B.A. Prentice, D. Sllberman, J.M. Ondov, A.H. Biermann, R.C. Ragainl, A.R. McFarl, Physical and morphological studies of size-classified coal fly ash, Environ. Sci. Technol. 12 (1978) 447–451.

[54] M.S. Sultana, A. Rahman, Characterization of calcined sugarcane bagasse sugarcane waste ash for industrial use, in: International Conference on Mechanical, Industrial and Materials Engineering 2013, 2013, pp. 508–513.

[55] Y. Kuwahara, T. Ohmichi, K. Mori, I. Katayama, H. Yamashita, Synthesis of zeolite from steel slag and its application as a support of nano-sized TiO_2 photocatalyst, J. Mater. Sci. 43 (2008) 2407–2410.

[56] A. Molina, C. Poole, A comparative study using two methods to produce zeolites from fly ash, Miner. Eng. 17 (2004) 167–173.

[57] A. Taufiq, P. Hidayat, A. Hidayat, Modified coal fly ash as low cost adsorbent for removal reactive dyes from batik industry, MATEC Web of Conferences 154 (2018), 01037.

[58] S.O. Bada, S. Potgieter-Vermaak, Evaluation and treatment of coal fly ash for adsorption application, Leonardo El J. Pract. Technol. 7 (2008) 37–48.

[59] H.A. Smail, K.M. Shareef, Z.H. Ramli, An eco-friendly process for removal of lead from aqueous solution, Mod. Appl. Sci. 11 (2017) 47.

[60] T.J. Mays, A new classification of pore sizes, Stud. Surf. Sci. Catal. 160 (2007) 57–62.

[61] M.S. Sultana, A. Rahman, Characterization of calcined sugarcane bagasse sugarcane waste ash for industrial use, International Conference on Mechanical, Industrial and Materials Engineering 2013 (2013) 508–513.

[62] M. Visa, Synthesis and characterization of new zeolite materials obtained from fly ash for heavy metals removal in advanced wastewater treatment, Powder Technol 294 (2016) 338–347.

[63] M.M. Treacy, J.B. Higgins, Collections of Simulated XRD Powder Patterns for Zeolites, first ed., Natherlands, Amsterdam, 2001.

[64] S.H. da Silva Filho, P. Vinaches, H.L.G. Silva, S.B.C. Pergher, LTA zeolite synthesis using natural materials and its evaluation by green star methodology, SN Appl. Sci. 2 (2020) 1–6.

[65] P. Zhang, W. Liao, A. Kumar, Q. Zhang, H. Ma, Characterization of sugarcane bagasse ash as a potential supplementary cementitious material: comparison with coal combustion fly ash, J. Clean. Prod. 277 (2020) 123834.

[66] P. Chindaprasirt, W. Kroehong, N. Damrongwiriyanupap, W. Suriyo, C. Jaturapitakkul, Mechanical properties, chloride resistance and microstructure of portland fly ash cement concrete containing high volume bagasse ash, J. Build. Eng. 31 (2020) 101415.

[67] G. Xu, X. Shi, Characteristics and applications of fly ash as a sustainable construction material: a state-of-the-art review, Resour. Conserv. Recycl. 136 (2018) 95–109.

[68] Y.R. Lee, J.T. Soe, S. Zhang, J.W. Ahn, M.B. Park, W.S. Ahn, Synthesis of nanoporous materials via recycling coal fly ash and other solid wastes: a mini review, Chem. Eng. J. 317 (2017) 821–843.

[69] S.M. Al-Jubouri, H.A. Sabbar, H.A. Lafta, B.I. Waisi, Effect of synthesis parameters on the formation 4a zeolite crystals: characterization analysis and heavy metals uptake performance study for water treatment, Desalination Water Treat 165 (2019) 290–300.

[70] S. Alfaro, C. Rodríguez, M.A. Valenzuela, P. Bosch, Aging time effect on the synthesis of small crystal LTA zeolites in the absence of organic template, Mater. Lett. 61 (2007) 4655–4658.

[71] K.S. Hui, C.Y.H. Chao, Effects of step-change of synthesis temperature on synthesis of zeolite 4A from coal fly ash, Microporous Mesoporous Mater 88 (2006) 145–151.

[72] B.A. Holmberg, H. Wang, J.M. Norbeck, Y. Yan, Controlling size and yield of zeolite Y nanocrystals using tetramethylammonium bromide, Microporous Mesoporous Mater 59 (2003) 13–28.

[73] P. Khaosomboon, K. Khuanmar, P. Weerayutsil, Synthesis of zeolite-A and zeolite-Y using silica gel waste as silica source and modifying with Fe, Int. J. Eng. Technol. 7 (2018) 1376.

[74] S. Hashemian, S.H. Hosseini, H. Salehifar, K. Salari, Adsorption of Fe(III) from aqueous solution by Linde Type-A zeolite, AJAC 4 (2013) 123–126.

[77] D.E. Beving, C.R. O'Neill, Y. Yan, Hydrophilic and antimicrobial low-silica-zeolite LTA and high-silica-zeolite MFI hybrid coatings on aluminum alloys, Microporous Mesoporous Mater 108 (2008) 77–85.

[78] A.R. Loiola, J.C.R.A. Andrade, J.M. Sasaki, L.R.D. da Silva, Structural analysis of zeolite NaA synthesized by a cost-effective hydrothermal method using kaolin and its use as water softener, J. Colloid Interface Sci. 367 (2012) 34–39.

[79] Z. Jiang, J. Yang, H. Ma, X. Ma, J. Yuan, Synthesis of pure NaA zeolites from coal. fly ashes for ammonium removal from. aqueous solutions, Clean Technol. Environ. Policy. 18 (2016) 629–637.

[80] X. Ren, L. Xiao, R. Qu, S. Liu, D. Ye, H. Song, W. Wu, C. Zheng, X. Wu, X. Gao, Synthesis and characterization of a single phase zeolite A using coal fly ash, RSC Adv 8 (2018) 42200–42209.

[81] C.A. Ríos Reyes, Synthesis of Zeolites from Geological Materials and Industrial Wastes for Potential Application in Environmental Problems, University of Wolverhampton, English, 2008.

[82] V. Somerset, L. Petrik, E. Iwuoha, Alkaline hydrothermal conversion of fly ash precipitates into zeolites 3: the removal of mercury and lead ions from wastewater, J. Environ. Manage. 87 (2008) 125–131.

[83] H. Cho, D. Oh, K. Kim, A study on removal characteristics of heavy metals from aqueous solution by fly ash, J. Hazard. Mater. 127 (2005) 187–195.

[84] A. Threepanich, P. Praipipat, Powdered and beaded lemon peels-doped iron (III) oxide-hydroxide materials for lead removal applications: synthesis, characterizations, and lead adsorption studies, J. Environ. Chem. Eng. 9 (2021) 106007.

[85] H. Xu, L. Wu, T. Shi, W. Liu, S. Qi, Adsorption of acid fuchsin onto LTA-type zeolite derived from fly ash, Sci. China Technol. Sci. 57 (2014) 1127–1134.

[86] H.A. Hani, S.R. Tewfik, M.H. Sorour, N.A. Monem, Acid washing of zeolite A: performance assessment and optimization, J Am Sci 6 (2010) 261–271.

[87] T. Motsi, N.A. Rowson, M.J.H. Simmons, Adsorption of heavy metals from acid mine drainage by natural zeolite, Int. J. Miner. Process. 92 (2009) 42–48.

[88] M. Karatas, Removal of Pb(II) from water by natural zeolitic tuff: kinetics and thermodynamics, J. Hazard. Mater. 199–200 (2012) 383–389.

[89] W. Yang, X. Wang, Y. Tang, Y. Wang, C. Ke, S. Fu, Layer by layer assembly of nanozeolite based on polymeric microsphere: zeolite coated sphere and hollow zeolite sphere, J. Macromol. Sci. A. 39 (2002) 509–526.

[90] T. Cheng, C. Chen, R. Tang, C.H. Han, Y. Tian, Competitive adsorption of Cu, Ni, Pb, and Cd from aqueous solution onto fly ash-based linde F(K) Zeolite, IJCCE 37 (2018) 61–72.

[91] R.-L. Tseng, F.-C. Wu, Inferring the favorable adsorption level and the concurrent multi-stage process with the Freundlich constant, J. Hazard. Mater. 155 (2008) 277–287.

[92] Y. Liu, C. Yan, Z. Zhang, H. Wang, S. Zhou, W. Zhou, A comparative study on fly ash, geopolymer and faujasite block for Pb removal from aqueous solution, Fuel 185 (2016) 181–189.

[93] B. Shah, C. Mistry, A. Shah, Seizure modeling of Pb (II) and Cd (II) from aqueous solution by chemically modified sugarcane bagasse fly ash: isotherms, kinetics, and column study, Environ. Sci. Pollut. Res. 20 (2013) 2193–2209.

[94] A.M. Aljeboree, A.N. Alshirifi, A.F. Alkaim, Kinetics and equilibrium study for the adsorption of textile dyes on coconut shell activated carbon, Arab. J. Chem. 10 (2017) S3381–S3393.

[95] W. Li, D. Chen, F. Xia, J.Z.Y. Tan, P.P. Huang, W.G. Song, N.M. Nursam, R.A. Caruso, Extremely high arsenic removal capacity for mesoporous aluminium magnesium oxide composites, Environ. Sci. Nano. 3 (2016) 94–106.

[96] W. Zou, R. Han, Z. Chen, Z. Jinghua, J. Shi, Kinetic study of adsorption of Cu (II) and Pb (II) from aqueous solutions using manganese oxide coated zeolite in batch mode, Colloids Surf. A Physicochem. Eng. Asp. 279 (2006) 238–246.

[97] P. Xing, C. Wang, B. Ma, Y. Chen, Removal of Pb (II) from aqueous solution using a new zeolite-type absorbent: potassium ore leaching residue, J. Environ. Eng. 6 (2018) 7138–7143.

[98] X. Huang, H. Zhao, G. Zhang, J. Li, Y. Yang, P. Ji, Potential of removing Cd (II) and Pb (II) from contaminated water using a newly modified fly ash, Chemosphere 242 (2020) 125148.

[99] M. Irannajad, H.K. Haghighi, Removal of Co^{2+}, Ni^{2+}, and Pb^{2+} by manganese oxide-coated zeolite: equilibrium, thermodynamics, and kinetics studies, Clays Clay Miner 65 (2017) 52–62.

[100] Z. Li, L. Wang, J. Meng, X. Liu, J. Xu, F. Wang, P. Brookes, Zeolite-supported nanoscale zero-valent iron: new findings on simultaneous adsorption of Cd (II), Pb (II), and as (III) in aqueous solution and soil, J. Hazard. Mater. 344 (2018) 1–11.

[101] X. Fan, H. Liu, E. Anang, D. Ren, Effects of electronegativity and hydration energy on the selective adsorption of heavy metal ions by synthetic nax zeolite, Mater 14 (2021).

[102] B. Sigfusson, A.A. Meharg, S.R. Gislason, Regulation of arsenic mobility on basaltic glass surfaces by speciation and pH, Environ. Sci. Technol. 42 (2008) 8816–8821.

[103] G. Chen, L. Shi, Removal of Cd(II) and Pb(II) ions from natural water using a low-cost synthetic mineral: behavior and mechanisms, RSC Advances 7 (2017) 43445–43454.

[104] N. Pangan, S. Gallardo, P. Gaspillo, W. Kurniawan, H. Hinode, M. Promentilla, Hydrothermal synthesis and characterization of zeolite A from corn (*zea mays*) stover ash, Mater 14 (2021) 4915.

[105] C.W. Purnomo, C. Salim, H. Hinode, Synthesis of pure Na-X and Na-A zeolite from bagasse fly ash, Microporous Mesoporous Mater 162 (2012) 6–13.

[106] H.I. Abdel-Shafy, M.S.M. Mansour, Solid waste issue: sources, composition, disposal, recycling, and valorization, Egypt, J. Pet. 27 (2018) 1275–1290.

[107] D. Hoornweg, P. Bhada-Tata, A global review of solid waste management - review, global management, solid waste, World Bank Urban Development Series Knowledge Papers 1 (2012) 1–116.

[108] C. Wang, J. Li, X. Sun, L. Wang, X. Sun, Evaluation of zeolites synthesized from fly ash as potential adsorbents for wastewater containing heavy metals, J. Environ. Sci. 21 (2009) 127–136.

[109] O. Marinina, M. Nevskaya, I. Jonek-Kowalska, R. Wolniak, M. Marinin, Recycling of coal fly ash as an example of an efficient circular economy: a stakeholder approach, Energies 14 (2021) 3597.